Global Change Biology **WILEY**

Coordination of photosynthetic traits across soil and climate gradients

Andrea C. Westerband[1] | Ian J. Wright[2,1] | Vincent Maire[3] | Jennifer Paillassa[3] |
Iain Colin Prentice[1,4,5] | Owen K. Atkin[6] | Keith J. Bloomfield[4] |
Lucas A. Cernusak[7] | Ning Dong[1,4] | Sean M. Gleason[8] |
Caio Guilherme Pereira[9] | Hans Lambers[10] | Michelle R. Leishman[1] |
Yadvinder Malhi[11] | Rachael H. Nolan[2]

[1]Faculty of Science and Engineering, School of Natural Sciences, Macquarie University, North Ryde, New South Wales, Australia

[2]Hawkesbury Institute for the Environment, Western Sydney University, Penrith, New South Wales, Australia

[3]Département des Sciences de l'environnement, Université du Québec à Trois-Rivières, Trois-Rivières, Québec, Canada

[4]Georgina Mace Centre for the Living Planet, Imperial College London, Ascot, UK

[5]Department of Earth System Science, Tsinghua University, Beijing, China

[6]Australian Research Council Centre of Excellence in Plant Energy Biology, Research School of Biology, The Australian National University, Canberra, Australian Capital Territory, Australia

[7]College of Science and Engineering, James Cook University, Cairns, Queensland, Australia

[8]USDA-ARS Water Management and Systems Research Unit, Fort Collins, Colorado, USA

[9]Department of Civil and Environmental Engineering, Massachusetts Institute of Technology, Cambridge, Massachusetts, USA

[10]School of Biological Sciences, University of Western Australia, Perth, Western Australia, Australia

[11]School of Geography and the Environment, Environmental Change Institute, University of Oxford, Oxford, UK

Correspondence
Andrea C. Westerband, Faculty of Science and Engineering, School of Natural Sciences, Macquarie University, North Ryde, NSW 2109, Australia.
Email: andreawesterband@gmail.com

Abstract

"Least-cost theory" posits that C_3 plants should balance rates of photosynthetic water loss and carboxylation in relation to the relative acquisition and maintenance costs of resources required for these activities. Here we investigated the dependency of photosynthetic traits on climate and soil properties using a new Australia-wide trait dataset spanning 528 species from 67 sites. We tested the hypotheses that plants on relatively cold or dry sites, or on relatively more fertile sites, would typically operate at greater CO_2 drawdown (lower ratio of leaf internal to ambient CO_2, $C_i:C_a$) during light-saturated photosynthesis, and at higher leaf N per area (N_{area}) and higher carboxylation capacity ($V_{cmax\,25}$) for a given rate of stomatal conductance to water vapour, g_{sw}. These results would be indicative of plants having relatively higher water costs than nutrient costs. In general, our hypotheses were supported. Soil total phosphorus (P) concentration and (more weakly) soil pH exerted positive effects on the N_{area}–g_{sw} and $V_{cmax\,25}$–g_{sw} slopes, and negative effects on $C_i:C_a$. The P effect strengthened when the effect of climate was removed via partial regression. We observed similar trends with increasing soil cation exchange capacity and clay content, which affect soil nutrient availability, and found

wileyonlinelibrary.com/journal/gcb | **1**

that soil properties explained similar amounts of variation in the focal traits as climate did. Although climate typically explained more trait variation than soil did, together they explained up to 52% of variation in the slope relationships and soil properties explained up to 30% of the variation in individual traits. Soils influenced photosynthetic traits as well as their coordination. In particular, the influence of soil P likely reflects the Australia's geologically ancient low-relief landscapes with highly leached soils. Least-cost theory provides a valuable framework for understanding trade-offs between resource costs and use in plants, including limiting soil nutrients.

1 | INTRODUCTION

Photosynthesis is a fundamental process in the global carbon cycle, governing flows of energy (Friend et al., 2009; Smith & Dukes, 2013). Broad-scale influences of site climate on photosynthesis and associated traits have been widely reported. For example, leaf nitrogen concentration on an area basis (N_{area}) and area-based rates of light-saturated photosynthesis, A_{sat}, are typically higher on relatively arid sites (Wright et al., 2005). Central to determining rates of photosynthesis is the internal concentration of CO_2 within leaves (C_i), as the ratio of intercellular to atmospheric CO_2 concentration (C_i:C_a) represents the balance between CO_2 demand (from the photosynthetic carboxylating enzyme, Rubisco) and supply (via stomata) during photosynthesis. Typically, C_i:C_a corresponding with A_{sat} shows clear patterning with a variety of climate variables, being generally lower at arid, high-altitude and cold sites (Cornwell et al., 2018; Dong et al., 2020; Prentice et al., 2011, 2014). Carboxylation capacity (V_{cmax}) considered at ambient temperatures tends to be higher at warmer sites (Dong et al., 2022) and, at least within-species, is generally higher in summer than in winter (Bloomfield et al., 2018). Conversely, V_{cmax} normalized to a standard temperature (commonly 25°C) tends to be lower in summer than in winter (Bloomfield et al., 2018; Hikosaka et al., 2007; Lin et al., 2013) and declines with increasing growth temperature (Dong et al., 2017; Scafaro et al., 2017; Togashi et al., 2018). Finally, stomatal conductance to water, g_{sw}, shows little patterning with site climate, at least at a global scale: individually or together, site temperature and precipitation explain <1% variation in g_{sw} in the global trait dataset of Wright, Reich, et al. (2004). Within C_3 woody angiosperms measured across major terrestrial biomes, there is no relationship between g_{sw} and either mean annual temperature (MAT), photosynthetically active radiation (PAR), or atmospheric vapor pressure deficit (VPD) (Murray et al., 2019, 2020).

Broad-scale influences of soil properties on photosynthetic traits are less well documented but this area of research is growing. Maire et al. (2015) found that A_{sat} increased with increasing soil pH and decreased weakly with increasing soil organic C concentration but had no relationship with soil N or available P concentration.

N_{area} is higher on sites with high soil pH (Dong et al., 2020; Maire et al., 2015) and negatively correlated with soil organic C and soil total N concentrations, albeit weakly (Maire et al., 2015). Ordoñez et al. (2009) reported higher mass-based nitrogen concentrations at sites with faster N-mineralization rates (argued to be a more relevant index of plant-available N than soil total N concentration) but found no relationship between N_{area} and N-mineralization rate due to a concomitant increase in leaf area per unit mass (specific leaf area, SLA), where N_{area} is N_{mass} divided by SLA. Dong et al. (2020) reported lower C_i:C_a on high pH soils, as did Cornwell et al. (2018) and Paillassa et al. (2020). Paillassa et al. (2020) explored the role of soil textural properties and reported higher V_{cmax} coupled with higher g_{sw} on sites with high soil silt content, lower C_i:C_a on deeper soils, and higher C_i:C_a in areas of high soil silt content, the last of which was also reported by Cornwell et al. (2018). g_{sw} is higher on soils with low plant-available P concentration (Maire et al., 2015), although studies on soil P effects are scarce.

Soil pH, often described as a "master soil variable," has emerged as an important explanatory variable in several studies of plant trait variation. Globally, soil pH tends to be higher at more arid than at mesic sites (Slessarev et al., 2016), although in Australia acid soils also occur at arid sites, likely owing to its low-relief landscape and the predominance of highly leached, ancient soils (Kooyman et al., 2017). Previous studies have worked to decouple the effects of pH and aridity. Presumably, the effect of pH on photosynthetic traits relates to its influence on soil nutrient availability: broadly speaking, nutrient availabilities are highest at mid-range pH values and lowest on extremely alkaline or acid soils. This can occur via changes in solubility and oxidation states (Lambers & Oliveira, 2019), enzymatic activity (Sinsabaugh et al., 2008; Sinsabaugh & Follstad Shah, 2012) and shifts in the activity and diversity of soil microorganisms involved in nutrient cycling (Fierer & Jackson, 2006; Lauber et al., 2008). Hence, N and P availability are generally highest at intermediate levels of soil pH, driving shifts in key plant functions, including photosynthesis.

"Least-cost" theory (Wright et al., 2003) is a framework for understanding the coordination of water and nutrient use during photosynthesis, and how it varies with site climate and soil properties.

Under this theory, photosynthesis is conceptualized as a production process with two key inputs, N and water, which are associated with V_{cmax} and the transpiration pathway, respectively. Based on standard microeconomic theory for a two-factor production process, the optimal balance of these inputs—indicating the lowest total cost for a given level of production—is set by the ratio of the *unit costs* of the two resources. A key concept of the theory is *substitutability*: in principle, plants can economize on water use by "spending" more on leaf N (i.e., all else being equal, higher N_{area} at a given g_{sw} results in higher V_{cmax} and hence lower $C_i:C_a$), or economize on N use by operating at a higher g_{sw} or transpiration rate. Thus, the approach integrates the single-resource concepts of photosynthetic nitrogen-use efficiency and water-use efficiency (Field et al., 1983; Lambers & Oliveira, 2019; Smith et al., 1997).

Briefly summarizing, the following are key assumptions from least-cost theory (Prentice et al., 2014; Wang et al., 2017; Wright et al., 2003): (1) the unit cost for carboxylation or N_{area} is set by the combined costs of acquiring soil nutrients needed for photosynthetic enzymes and the respiratory costs of building and maintaining enzyme function (e.g., protein turnover); (2) soil nutrients are more expensive to acquire when at lower availability (e.g., from higher root construction costs; more carbon traded for nutrients with mycorrhizas; higher costs associated with producing root exudates, such as carboxylates or phosphatases); (3) the unit cost for transpiration is set by the cost of acquiring soil water and the respiratory costs of maintaining functional sapwood; (4) available soil water and VPD affect plant water costs but also plant water demands, as transpiration is the product of g_{sw} and VPD; (5) temperature affects Rubisco kinetics, which influences carboxylation costs (as described above), and also the viscosity of water which influences water costs; and finally, (6) elevation affects the saturated vapor pressure of water and hence VPD (influencing water costs), and also gas partial pressures (Körner et al., 1991), ultimately influencing the use of CO_2 versus O_2 by Rubisco and therefore carboxylation. Taken together, the optimum balance between resource investments in transpiration and carbon assimilation should thus depend both on soil properties and climate.

Assuming that site properties are the first-order controls on resource unit costs, typical $V_{cmax\,25}-g_{sw}$ and $N_{area}-g_{sw}$ ratios—and also $C_i:C_a$—should vary predictably across environmental gradients (and, conversely, there should be convergence in these traits among co-occurring species). With successive iterations of least-cost theory, the predictions have shifted from qualitative to quantitative (at least in regards to climate), with support accumulating at regional and global scales. Wright et al. (2003) and Prentice et al. (2014) observed, as predicted, that species from more arid or cooler sites in eastern Australia typically operate with higher N_{area} and $V_{cmax\,25}$ at a given g_{sw}, and at lower $C_i:C_a$. Wang et al. (2017) generated quantitative predictions for the independent effects of site temperature, aridity (VPD), and elevation on $C_i:C_a$ which were confirmed using a global dataset derived from leaf $\delta^{13}C$ values (Cornwell et al., 2018). Dong et al. (2017) and Smith et al. (2019) have successfully used least-cost theory combined with "photosynthetic coordination" theory (Chen

et al., 1993; Maire et al., 2012; Von Caemmerer & Farquhar, 1981) to predict climate-driven patterns in $V_{cmax\,25}$.

Here, we further investigate the effects of soil properties, primarily pH and total phosphorus (hereafter, P) concentration but also additional proxies for fertility, in driving photosynthetic coordination at a continental scale. In a global study (Paillassa et al., 2020), we reported that plants on neutral to moderately alkaline soils (pH up to 8) had higher $V_{cmax\,25}-g_{sw}$, higher $N_{area}-g_{sw}$, and lower $C_i:C_a$ than plants on relatively acidic soils (pH as low as 4), and that plants on deeper soils and soils with greater silt content had lower $V_{cmax\,25}-g_{sw}$, lower $N_{area}-g_{sw}$, and higher $C_i:C_a$ than plants on shallow soils with little silt. These results were interpreted as most likely reflecting lower unit costs for acquiring water on silt-rich and deep soils, and lower unit costs for acquiring N on higher pH soils. Few studies have investigated the role of soil pH in driving trait coordination, despite its importance for regulating nutrient availability. In that previous study, climate and soil data were derived from global gridded datasets. In the present study, we instead use a combination of measured and gridded soil data and, importantly, we purposefully shift the focus to soil P, a key limiting nutrient for photosynthesis (Domingues et al., 2010; Peng et al., 2021; Reich et al., 2009).

Phosphorus plays a key role in leaf function in relation to P-rich bioenergetic molecules (ATP, NADP, etc), Calvin–Benson cycle intermediates (e.g., ribulose-1,5-bisphosphate), membrane lipids, and nucleic acids. On deeply weathered and infertile soils, including those in Australia but also the tropics, P is a key limiting nutrient for plant productivity, and geographic variation in soil P delineates native vegetation communities (Beadle, 1954, 1966; Kooyman et al., 2017; Laliberté et al., 2014; Vitousek, 1984). Here we address the aforementioned knowledge gaps, combining published and unpublished datasets with de novo photosynthetic measurements, building a comprehensive photosynthetic trait database for Australian native plants (536 species from 67 sites, Figure S1).

Our aims were to understand the manner in which soils—and to a lesser extent climate—have driven the coordination of photosynthetic traits, and to characterize trait–environment relationships, focusing on soil pH, soil total P concentration, mean annual precipitation (MAP), and MAT for the Australian flora. Better regional and global understanding of photosynthetic trait–environment relationships has the potential to improve existing global vegetation models by expanding on the environmental dependencies of traits. We focused on the effects of soil fertility via soil total P concentration and soil pH, both of which presumably influence the unit costs of N and carboxylation more so than water costs, and we tested a number of key predictions (Figure 1a). First, assuming—all else equal—that the unit costs of soil nutrients are lower on higher P soils or higher pH soils, we predicted that plants would increase their investment in N_{area} or V_{cmax} relative to g_{sw} in these situations, and operate at lower $C_i:C_a$. We note that while extremely high pH soils reduce soil nutrient availability (Lambers & Oliveira, 2019), Australian soils are predominantly acidic compared with other arid regions of the world (Slessarev et al., 2016). Second, we predicted the same trait shifts (higher $V_{cmax}-g_{sw}$, higher $N_{area}-g_{sw}$, and lower $C_i:C_a$) in arid compared with wetter sites and on relatively
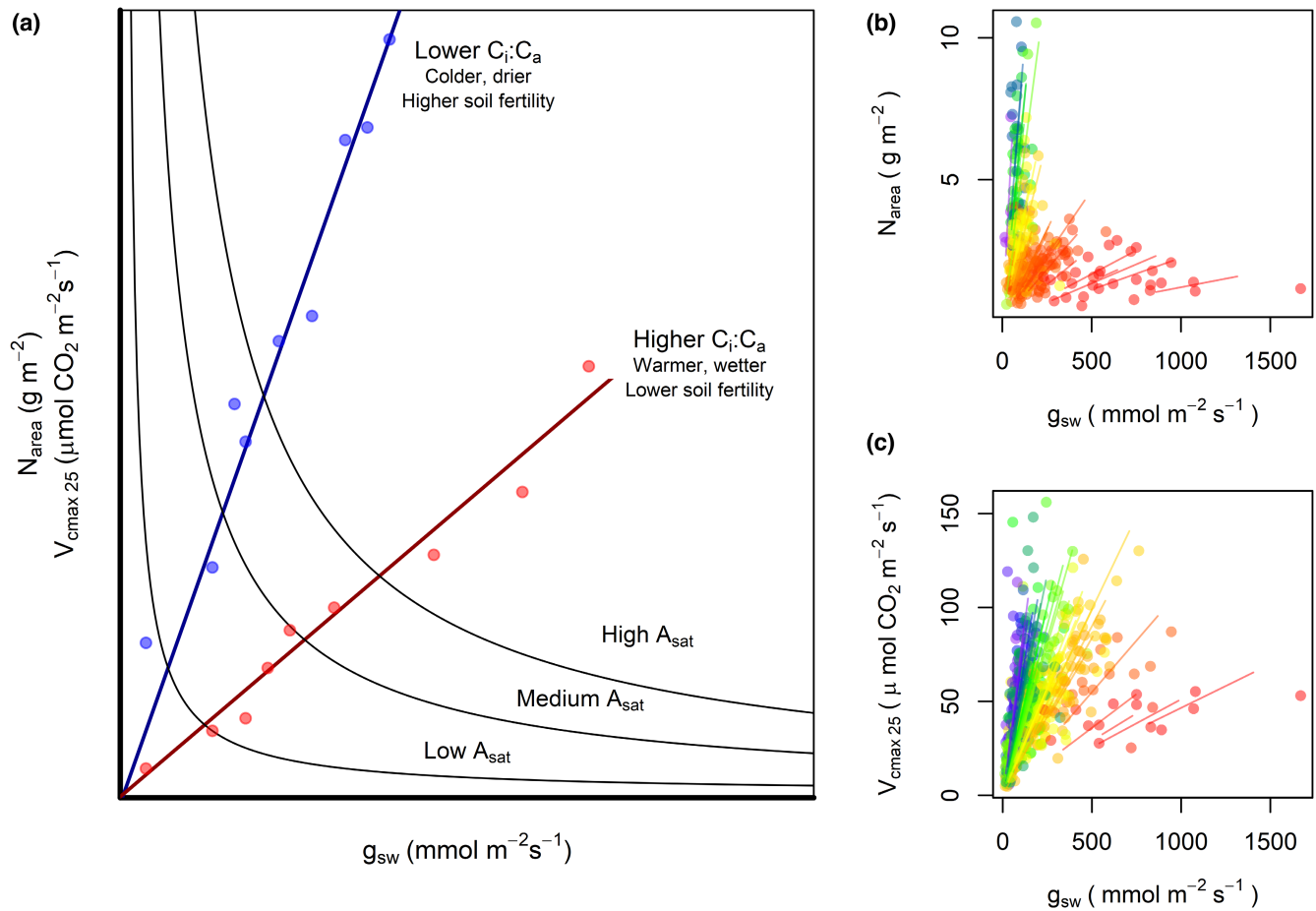
FIGURE 1 An approach based on least-cost theory for understanding the co-optimization of photosynthetic traits in relation to site properties. (a) The theory predicts that the optimal ratio of water and nitrogen (N) use during light-saturated photosynthesis (A_{sat}) depends on their relative costs of acquisition and use. Nitrogen use is represented by leaf N content per unit area (N_{area}) and carboxylation capacity ($V_{cmax\,25}$). Water use is represented by stomatal conductance (g_{sw}). Blue dots represent site conditions where water costs are relatively greater than N costs, or alternatively, where N costs are relatively lower than water costs. $C_i:C_a$ is the ratio of leaf internal to ambient CO_2 concentration and mediates the relationship between N use (and carboxylation) and water use. In this study, we found significant site-level variation in (b) photosynthetic N use versus water use, and (c) carboxylation versus water use, which we quantified using a slope fitted to a set of co-occurring species at each site, where each point represents a species-site mean. Each line was "forced" through the origin. Blue and purple tones represent sites with higher water costs and simultaneously lower N costs, while orange and red tones represent lower water costs and simultaneously higher N costs.

colder compared with warmer sites. These predictions arise from the assumption that the unit cost of water is greater at low rainfall and high VPD, and that temperature affects the unit costs of both carboxylation and photosynthetic water use (Prentice et al., 2014), as described above. The results from this study will be of global significance, as they will clarify whether trait coordination patterns observed at a global scale are consistent at a continental scale, in the context of locally relevant soil properties.

2 | MATERIALS AND METHODS

2.1 | Study system

Australia is highly suited for this line of inquiry as there is wide environmental variation in both soils and climate. The central portion of the continent (ca. 70% by land area) is arid to semi-arid, while coastal regions vary from Mediterranean in the south to southwest, cool temperate in the south, temperate to tropical in the east, and wet–dry tropics in the far north. Although Australian soils are on the whole ancient and nutrient-poor (He et al., 2021; Kooyman et al., 2017; Viscarra Rossel & Bui, 2016), higher-nutrient soils punctuate the landscape (de Caritat et al., 2011; Viscarra Rossel & Bui, 2016) and the Great Dividing Range, which runs 3500 km north to south, approximately parallel to the east coast of Australia, divides the mesic coastal regions from the arid interior. Furthermore, although much of Australia has acidic soil, calcareous soils with high pH are also present across wide areas (de Caritat et al., 2011), for example in southern Australia, resulting from repeated marine incursions beginning in the Miocene era (Northcote & Wright, 1982; Taylor, 1994). In this study, the majority of the sites were on acidic soils with low soil nutrient availability (Table S1), which is representative of Australia but also relevant to other, similarly leached regions of the world.

2.2 | Field data collection

Leaf trait data were collected on woody and non-woody plant species at three sites between December 2018 and March 2019: Kidman Springs Research Station (tropical savanna, sampled during the wet season; Northern Territory), Royal National Park (subtropical rainforest; New South Wales), and Mount Keira (subtropical rainforest; New South Wales). Latitude, longitude, and climate data for these sites can be found in Table S1. These sites were chosen to increase the number of samples within sites of moderately high total soil P concentrations and moderately high soil pH (Figure S2), compared with site coverage in our compilation of literature data, described below. Ten soil samples (to 30 cm depth) were collected at each site and air-dried prior to laboratory analyses (CSPB laboratory in Bibra Lake WA, Australia) of soil pH in $CaCl_2$ solution (Rayment & Lyons, 2011) and total soil P concentration via colorimetry, following Kjeldahl digestion (Rayment and Lyons Method 9A3b).

We sampled seven to 28 species per site, randomly selecting three to eight individuals per species and focusing on dominant woody and non-woody species (excluding C_4 plants). Photosynthetic traits were measured using a Li-6800 gas exchange system (Li-Cor Biosciences). Survey-style gas exchange measurements were made between 0800 and 1400 h on one leaf per plant. Young but fully expanded, undamaged leaves were sampled from the most sun-exposed portion of each canopy. We measured light-saturated (photosynthetic photon flux density of $1800\,\mu mol\,m^{-2}\,s^{-1}$) photosynthesis per unit area (A_{area}, $\mu mol\,CO_2\,m^{-2}\,s^{-1}$) at an atmospheric CO_2 concentration of $400\,\mu mol\,mol^{-1}$, allowing leaves to remain in the chamber for several minutes. Leaf temperatures were initially set to 25°C, although in many cases the temperature had to be increased above this to prevent condensation in the cuvette. Mean leaf temperature was 29°C with 95% of measurements made between 25 and 35°C; relative humidity varied between 40 and 80%. We also recorded stomatal conductance to water vapor (g_{sw}, $mmol\,m^{-2}\,s^{-1}$) associated with light-saturated photosynthesis, and the ratio of internal to ambient CO_2 concentration (C_i:C_a, unitless). We note that gas exchange rates are sensitive to plant water status and can exhibit pronounced temporal (e.g., diurnal, seasonal) variation. By measuring photosynthesis and stomatal conductance in light-saturated leaves at a controlled temperature and humidity, we reduced the amount of variation in the data by creating favorable conditions for photosynthesis inside the cuvette.

We also collected five or more outer canopy leaves per plant, sampling from multiple branches up to 10 m above the ground, using an extendable pole pruner. Leaves were scanned to estimate leaf area, dried at 60°C for a minimum of 72 h and weighed to calculate leaf mass per area (LMA, $g\,m^{-2}$). Samples were analyzed for leaf N concentration (% mass basis) by the Stable Isotope Core Laboratory at Washington State University, USA using an elemental analyzer (ECS 4010, Costech Analytical). Leaf N per area (N_{area}; $g\,m^{-2}$) was calculated as $N_{area} = N_{mass} \times SLA^{-1}$.

2.3 | Data compilation

2.3.1 | Trait data

We compiled field-measured photosynthetic trait data from published and unpublished studies that employed similar standard methods to those described above, that is, light-saturated photosynthesis measured on young but fully expanded, undamaged "sun" leaves at ambient atmospheric CO_2 concentration, and relative humidity between 40 and 80%. See Table S2 for a full list of source publications, noting that some of the trait data included herein are not published. Further details regarding our field methods can be found below. For inclusion, a dataset had to contain field-measured A_{sat}, g_{sw}, and C_i; where available we also extracted data for leaf temperature (T_{leaf}), LMA, and N_{area}. We estimated carboxylation capacity at a standardized temperature of 25°C ($V_{cmax\,25}$) following the one-point method (De Kauwe et al., 2016), which utilizes T_{leaf}, A_{sat}, and C_i. We consulted the original publication or contacted the data owners to determine the appropriate leaf temperature for studies where T_{leaf} was not reported. If $V_{cmax\,25}$ from a CO_2-response (A-C_i) curve was provided, we used these data rather than estimating $V_{cmax\,25}$ via the "one-point method" (De Kauwe et al., 2016); 179 measurements, or 6% of the original dataset. To ensure consistency in approach to estimating V_{cmax}, R_{day} (CO_2 evolution from mitochondria in the light) was estimated as 1.5% of V_{cmax}, following De Kauwe et al. (2016), rather than from reported estimates of field-measured leaf "dark" respiration (R_d, which were relatively scarce among the compiled datasets).

We visually inspected the data to find obvious errors (e.g., trait values <0; C_i:C_a >1) and outliers, conservatively excluding from the analyses any observations with $V_{cmax\,25}$ > 500 $\mu mol\,CO_2\,m^{-2}\,s^{-1}$, and g_{sw} > 3000 $mmol\,m^{-2}\,s^{-1}$. This resulted in the exclusion of nine observations (seven for $V_{cmax\,25}$, two for g_{sw}). These cut-offs were based on previously published studies (Smith et al., 2019; Wright, Reich, et al., 2004).

In combination with the de novo field measurements described above, we amassed a trait dataset for 3765 individuals of 528 species (85 families), sampled from 67 study sites (Figure S1 and Table S1). One hundred and fifty-two species occurred at more than one site. On average, 11 species were sampled per site, although this varied widely (Table S1). Species-mean trait values were calculated at each site, although subspecies were kept separate, when reported. Taxonomy followed The Plant List (accessed via http://www.plantminer.com/). Thirteen individuals could not be identified beyond the genus level but were still included, and 20 species had names that are taxonomically unresolved in The Plant List. The final dataset included a variety of growth forms (mostly trees and shrubs but 28 herbaceous species, or 4.5% of the dataset), primarily evergreen species, no winter-deciduous species, some drought-deciduous species such as *Toona ciliata* and *Melia azedarach*, and a mixture of N_2-fixing species (mostly Fabaceae but also Casuarinaceae and Zamiaceae) and non-N_2-fixing species (84% of the dataset). There were 10 gymnosperm species, distributed among five families (Araucariaceae,

Cupressaceae, Zamiaceae, Podocarpaceae, and Pinaceae). The original data compilation included five C_4 species from the genus *Atriplex* and *Triodia* (Amaranthaceae and Poaceae, respectively) but these were excluded from calculations of V_{cmax} as the one-point method is based on the Farquhar et al. ([1980](#)) model of C_3 photosynthesis.

2.3.2 | Climate and soil data

Long-term averages (1982–2002) of climate data (Table [S3](#)) were obtained for each site from the ANUClimate model (Hutchinson et al., [2009](#)) and TERN Ecosystem Modelling and Scaling Infrastructure (eMAST) data products (Hutchinson et al., [2009](#); Xu et al., [2015](#)), both of which provide Australia-wide coverage at 0.01° spatial resolution, 1970–2012 (https://www.tern.org.au/). We include a total of 21 soil and climate properties. Across the 68 study sites, MAT varied from 9.25 to 27.6°C, and MAP from 260 to 4390mm (Figure [S2](#)).

We had field-measured data for soil total P concentrations from 34 sites and for soil pH ($CaCl_2$) from 28 sites. Otherwise we extracted modelled estimates of soil total P concentration and pH ($CaCl_2$) from the TERN Soil and Landscape Grid of Australia (Grundy et al., [2015](#); Viscarra Rossel et al., [2014](#)) (https://data.csiro.au/), which offers Australia-wide gridded data at a resolution of 3 arc s (ca. 90×90 m pixels). We also extracted additional soil properties known to influence soil fertility, including soil texture, soil organic matter concentration, and cation exchange capacity (Table [S3](#)). In the combined dataset, soil total P concentration varied from 28.8 to 3790ppm ($mg\,kg^{-1}$), and pH from 3 to 9. There were two sites with exceptionally high (measured) soil P concentrations (Dorrigo National Park, NSW and Curtain Fig National Park, QLD); without these sites, maximum soil P concentration was 1786ppm.

2.4 | Statistical analyses

We report results from all models with $p < .1$, noting those with $.05 < p < .10$ as "marginally significant." All statistical analyses were carried out in R version 3.5.3 (R Development Core Team, [2017](#)).

2.4.1 | Testing predictions from least-cost theory

$V_{cmax\,25}$–g_{sw} and N_{area}–g_{sw} relationships at each site were summarized as standardized major axis (SMA) slopes fitted with no intercept term (i.e., "forced" through the origin), using untransformed data. These slopes, therefore, represent the average ratios of $V_{cmax\,25}$–g_{sw} and N_{area}–g_{sw} at each site (Wright et al., [2003](#)). We conducted a slope heterogeneity test to assess site differences, using "SMATR" for R (Warton et al., [2006](#)). Sites with low replication (<3 species per site) were left out from this analysis (two sites for $V_{cmax\,25}$ and three sites for N_{area}), resulting in 58 $V_{cmax\,25}$–g_{sw} slopes and 39 N_{area}–g_{sw} slopes.

Next, bivariate and multiple linear regression analyses were used to quantify the influence of soil and climate properties on C_i:C_a as well as the $V_{cmax\,25}$–g_{sw} and N_{area}–g_{sw} slopes. We tested how these traits varied in response to a total of 21 abiotic variables using bivariate regressions but were unable to include the full suite of predictors in the multiple regression due to multicollinearity and a lack of statistical power. For example, while VPD is often considered an important variable driving photosynthetic trait coordination (Paillassa et al., [2020](#)), in this study it was highly correlated with both MAP and MAT. Similarly, soil pH was correlated with soil N concentration, and soil P and N concentrations were correlated with one another (Figure [S3](#)). Therefore, we reduced the set of predictors in the multiple regression to focus on soil pH and soil P concentration, which were not correlated (Figure [S3](#)), and also MAP and MAT, which were only weakly (positively) correlated (Figure [S2](#)). We selected soil P rather than soil N because soil P is a more strongly limiting soil nutrient for plants within Australia (Beadle, [1954](#), [1966](#)). Soil pH and soil P were independently correlated with MAT and MAP in opposing directions: soil P concentration was negatively (albeit weakly) correlated with MAT and positively correlated with MAP, whereas soil pH was positively correlated with MAT and negatively correlated with MAP. In other words, relatively colder sites and sites with higher mean annual precipitation had a lower soil pH and higher soil total P concentration, on average (Figure [S2](#)). With the exception of C_i:C_a in the multiple regression, the dependent and independent variables were log_{10}-transformed prior to analyses to meet assumptions of normality.

From multiple regression analyses, we report the beta values for each predictor, that is, the regression weights for standardized variables, representing the change in the response variable (in standard deviations) associated with a change of one standard deviation in a given predictor, other predictors being held constant (Courville & Thompson, [2001](#); Pedhazur, [1997](#)). These partial effects were visualized with "added variable" (partial regression) plots, created using the avPlots function in the "car" package. Beta weight values (hereafter, β) were calculated using the regr function in the "yhat" package.

We also ran the above analyses after excluding species that were presumed to fix N_2 (Fabaceae, Casuarinaceae, Zamiaceae) as, on average, these species had notably higher leaf N_{mass} and N_{area} than non-fixing species ($p < .001$, Figure [S4](#)). However, the results (Figure [S5](#)) changed little compared with those from main analyses, the key difference being that soil P exerted a stronger, positive effect on the N_{area}–g_{sw} relationship. Our overall conclusions were not affected therefore these results are not discussed further.

2.4.2 | Quantifying climate and soil effects on photosynthetic traits

Climate and soil effects on individual photosynthetic traits were quantified via ordinary least squares (OLS) linear regressions, implemented using the lm function in base R. We investigated

relationships between the four focal plant traits ($C_i{:}C_a$, g_{sw}, $V_{cmax\,25}$, and N_{area}) and all 21 soil and climate variables. For this analysis, and for the subsequent partial regression analysis, we included additional traits known to covary with N_{area}, including P_{area}, LMA, and A_{area}. We also included photosynthetic phosphorus and nitrogen-use efficiency, PPUE and PNUE, respectively. In preliminary analyses, we tested quadratic fits between the focal traits and soil pH, finding that the quadratic models for $C_i{:}C_a$, N_{area}, and $V_{cmax\,25}$ had lower AIC (>2) than the linear models but added very little explanatory power: R^2 values of quadratic models ranged from 0.04 to 0.17, with a relative increase in $R^2 \leq 0.02$ for all traits. There was no improvement in the model fit for g_{sw}. Because our study sites were dominated by acidic soils (pH <7) we had no a priori reason to expect non-linear relationships between soil pH and nutrient availability, as typically occurs when comparing strongly acidic to strongly alkaline soils (Maire et al., 2015). Therefore, we did not expect non-linear relationships between soil pH and the focal traits and retained linear fits for all relationships. Leaf traits and abiotic variables were $\log_{10}$-transformed prior to the statistical analyses to satisfy assumptions of normality and homoscedasticity of the residuals.

We also evaluated trait–environment relationships using partial regression analyses on models that included either the four key predictors above (soil P, soil pH, MAP, and MAT) or seven predictors (soil P, soil pH, soil N, MAP, MAT, VPD, and radiation), which were selected because they are known to influence photosynthetic traits. Correlations between abiotic variables were visualized using the corrmat function in the "corrmat" package.

3 | RESULTS

3.1 | Trait variation

In the species-mean dataset, $V_{cmax\,25}$ varied ca. 27-fold (from 5.8 to 156 $\mu mol\,m^{-2}\,s^{-1}$, $n = 636$), g_{sw} varied ca. 150-fold (from 11.1 to 1670 $mmol\,m^{-2}\,s^{-1}$; $n = 664$), N_{area} ca. 19-fold (0.55 to 10.6 $g\,m^{-2}$; $n = 430$), and $C_i{:}C_a$ varied ca. fourfold (from 0.22 to 0.96; $n = 665$). The notably wider range in g_{sw} was due to one exceptionally high value for *Eucalyptus miniata* from Eamus and Prichard (1998). Excluding this g_{sw} would have resulted in a 90-fold variation; however, we had no basis on which to exclude this value. If variation in traits was compared in terms of the ratio of 97.5th to 2.5th percentiles, rather than maximum/minimum, variation in g_{sw} was comparable to that in other traits (ca. 22-fold). By comparison, the ratio of 97.5th to 2.5th percentiles for g_{sw} was ca. 23 in the global photosynthetic trait dataset of Maire et al. (2015).

3.2 | Bivariate tests of least-cost theory

$N_{area}–g_{sw}$ and $V_{cmax\,25}–g_{sw}$ slopes varied widely across sites (slope heterogeneity $p < .001$, Figure 1b,c) where steeper slopes indicate

that species are operating with higher $V_{cmax\,25}$ or N_{area} at a given rate of stomatal conductance to water vapor (Figure 1a). Contrary to our expectation, variations in these slopes were not associated with soil P concentration or soil pH in the bivariate regressions (Figure 2), and typically, the soil variables explained less than 5% of the variation in the slopes. Similarly, we found no association between the slope relationships and soil nitrogen (Soil N), bulk density of whole earth (BDW), soil organic carbon (SOC), and the soil textural properties. The only variable that significantly influenced the slope relationships was ECE, which exerted a positive effect on the slopes (Table S4), suggesting that higher ECE increased nutrient availability and reduced nutrient costs relative to water costs.

$C_i{:}C_a$ varied with both soil pH and soil P concentration in the expected manner, being lower on average at sites with high soil P concentrations (Figure 2i) or high pH (Figure 2j). $C_i{:}C_a$ also decreased with increasing ECE, increasing SOC, and increasing clay content (and increased with increasing silt and sand content) (Table S4), supporting our predictions (Figure 1a).

With regards to climate, the $N_{area}–g_{sw}$ and $V_{cmax\,25}–g_{sw}$ slopes were generally steeper at drier sites (Figure 2c,g) and at colder sites (Figure 2d,h), as predicted. For example, $N_{area}–g_{sw}$ slopes were ca. sixfold steeper at 300 mm MAP than at 3000 mm MAP (0.04 vs. 0.007, respectively), and $V_{cmax\,25}–g_{sw}$ slopes were ca. threefold steeper (0.52 vs. 0.19, respectively). From the bivariate regressions, MAP explained 31% and 24% of the variation in $N_{area}–g_{sw}$ and $V_{cmax\,25}–g_{sw}$ slopes, respectively (Table S4, Figure 2c,d). MAT explained 37% and 17% of the variation in $N_{area}–g_{sw}$ and $V_{cmax\,25}–g_{sw}$ slopes, respectively (Figure 2d,h).

Also as predicted, species at drier sites and at relatively colder sites operated at lower $C_i{:}C_a$ (Figure 2k,l). Using a standard moisture index, the ratio of MAP to potential evapotranspiration (Thornthwaite, 1948), gave similar results to using MAP alone (Table S4).

In general, climate variables explained a significantly greater percentage of the variation in the $N_{area}–g_{sw}$ and $V_{cmax\,25}–g_{sw}$ slopes ($0.005 \leq R^2 \leq 0.64$) than did the soil variables ($0.004 \leq R^2 \leq 0.24$). Similarly, a greater amount of variation in $C_i{:}C_a$ was explained by climate (max $R^2 = 0.12$) than by soil (max $R^2 = 0.08$).

3.3 | Multiple regression tests of least-cost theory

Multiple regression analyses revealed some distinct patterns from the bivariate regressions (Figure 3). Together, the four environmental variables explained 52% of variation in $N_{area}–g_{sw}$ slopes, 36% of variation in $V_{cmax\,25}–g_{sw}$ slopes, and 14% of variation in $C_i{:}C_a$. Comparing standardized regression coefficients (β values in Figure 3), MAP affected photosynthetic trait coordination more strongly than the three other environmental variables. The effect sizes for soil P concentration were of similar or slightly stronger magnitude to those for MAT, and notably weaker than the precipitation effects.
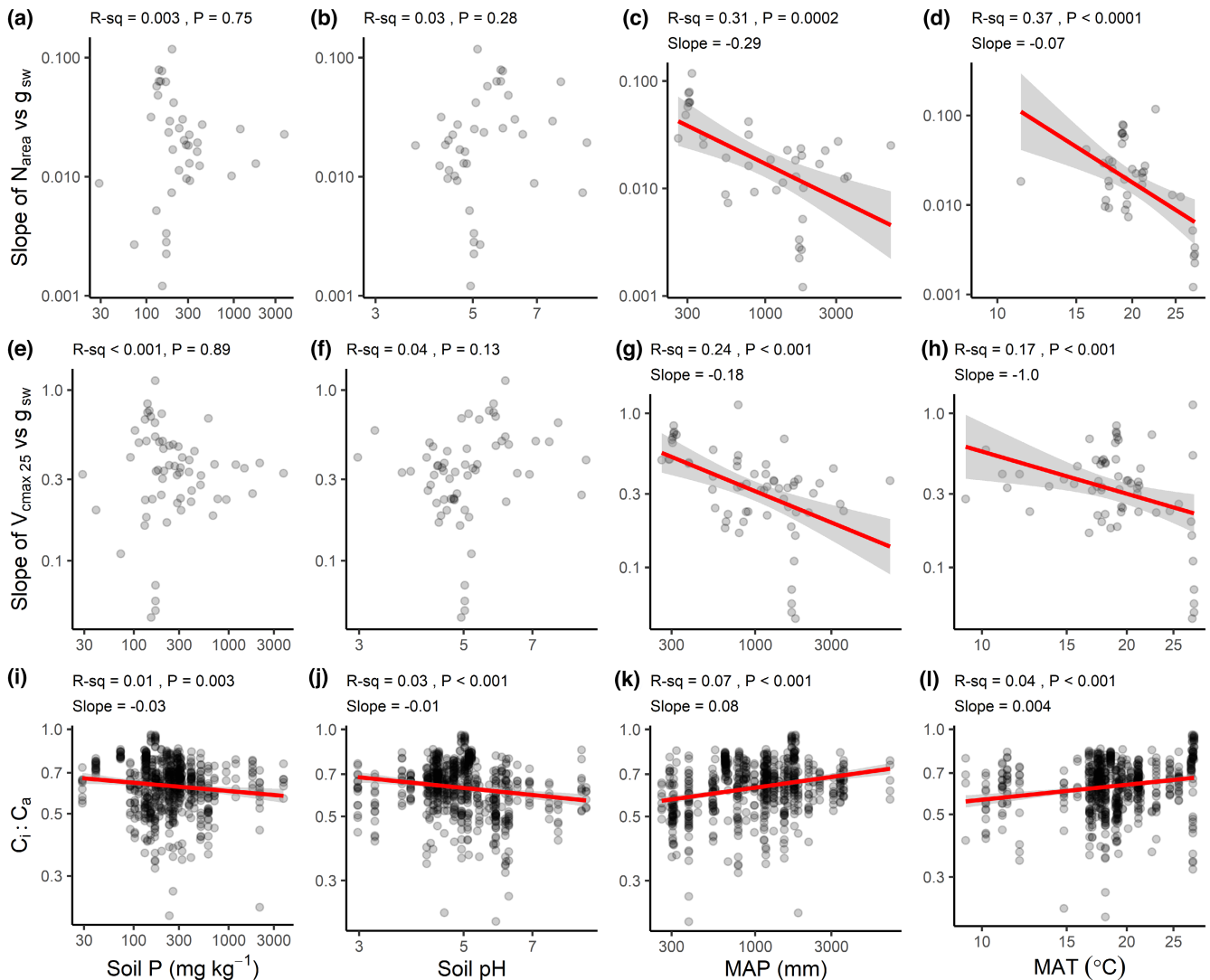
FIGURE 2 Linear regression plots of soil and climate effects on the (a)–(d) slope relationship between leaf nitrogen concentration (N) on an area basis, N_{area}, and stomatal conductance, g_{sw}, and the (e)–(h) slope relationship between photosynthetic carboxylation, $V_{cmax\,25}$, and g_{sw}. (i)–(l) Relationship between C_i:C_a and environmental variables. (a), (e), (i) Soil total phosphorus (Soil P, mg kg^{-1}) concentration, (b), (f), (j) Soil pH, (c), (g), (k) Mean annual precipitation (MAP, mm), and (d), (h), (l) Mean annual temperature (MAT, °C). Red lines represent trend lines with 95% confidence intervals in gray and are only shown for statistically significant (p-values <.05) relationships. Notice the logarithmic scale to the axes. See Figure 3 for partial regressions.

After controlling for variation in other predictors via partial regression, the effect of soil P concentration on the N_{area}–g_{sw} and $V_{cmax\,25}$–g_{sw} relationship slopes became stronger than what we observed in the OLS regression (i.e., $0.05 < p < .10$; Figure 3a,e). The soil P concentration effect on C_i:C_a (Figure 3i) was again negative, even when controlling for variation in MAT, MAP, and soil pH. These effects of soil P concentration were all in the predicted direction (Figure 1a). After controlling for variation in other predictors, soil pH still showed no association with N_{area}–g_{sw} and $V_{cmax\,25}$–g_{sw} relationship slopes (Figure 3b,f) or C_i:C_a (Figure 3j).

For both sets of slopes, models including all four predictors indicated that the MAP effect was strongly negative (in terms of β), and was stronger than that of MAT, soil P concentration and soil pH (Figure 3). That is, at a given MAT, soil P concentration or soil pH, species at drier sites typically operated with higher $V_{cmax\,25}$ or N_{area} at a given g_{sw}

(Figure 3c,g), and also typically had lower C_i:C_a (Figure 3k)—all trends consistent with the expectation that savings on photosynthetic water use can be achieved via increased investment in the N-rich carboxylating enzyme, Rubisco. The MAT effects on the N_{area}–g_{sw} and $V_{cmax\,25}$–g_{sw} slopes in the bivariate regressions were no longer apparent once other environmental variables were controlled (Figure 3d,h). By contrast, a positive MAT effect on C_i:C_a was observed when controlling for other variables, as was the case in the bivariate analysis (Figure 3l).

3.4 | Trait–environment relationships

We quantified relationships between environmental variables and plant photosynthetic traits including g_{sw}, $V_{cmax\,25}$, and N_{area}, but also additional traits known to covary with the focal variables
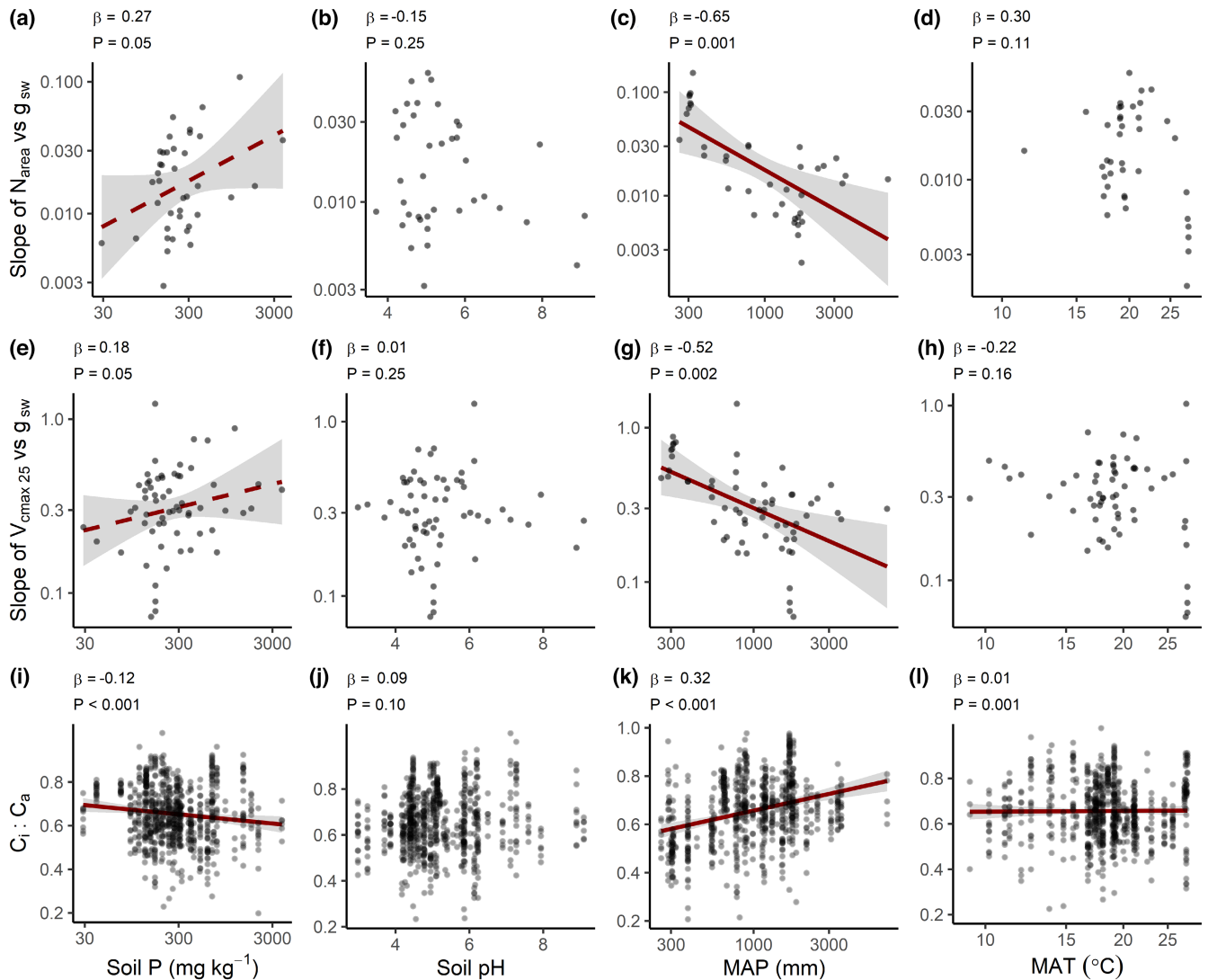
FIGURE 3 Partial regression plots from multiple linear regression of soil and climate effects on the (a)–(d) slope relationship between leaf nitrogen concentration (N) on an area basis, N_{area}, and stomatal conductance, g_{sw}, and the (e)–(h) slope relationship between photosynthetic carboxylation, $V_{cmax\,25}$, and g_{sw}. (i)–(l) Relationship between C_i:C_a and environmental variables. (a), (e), (i) soil total phosphorus (soil P, mg kg^{-1}) concentration, (b), (f), (j) soil pH, (c), (g), (k) mean annual precipitation (MAP, mm), and (d), (h), (l) mean annual temperature (MAT, °C). Points in gray represent partial regressions with standard errors in gray and dark red lines are shown only for statistically significant relationships, where solid lines have $p < .05$ and dashed lines are marginally significant ($.05 < p < .10$). p-values above each panel indicate the statistical significance of each variable in the multiple regression. Higher β values indicate a stronger effect size, where β values are the regression weights for standardized variables and represent the change in the slope value (in standard deviations) associated with a change of one standard deviation in a predictor while holding constant the value(s) of the other predictor(s).

(for the full suite of relationships, see Table S4). Species on low-P and on low-N soils tended to have higher g_{sw}, N_{area}, and $V_{cmax\,25}$ (Figure 4), whereas species on high pH soils (which in this dataset are expected to have higher soil nutrient availability) had higher $V_{cmax\,25}$ and higher N_{area} but exhibited no difference in g_{sw} (Figure 4b). The higher $V_{cmax\,25}$ and N_{area} on low-P soils were likely driven by higher LMA on low-P soils (Figure 4j, Table S4), as N_{area} was positively correlated with both LMA$_{25}$ ($r = 0.75$, $p < .001$) and $V_{cmax\,25}$ ($r = 0.37$, $p < .001$). Soil P concentration explained the highest percentage of the variation in $V_{cmax\,25}$ ($R^2 = 0.16$) whereas soil N concentration explained the highest percentage of the variation in N_{area} ($R^2 = 0.24$). On average, for a tenfold decrease in soil P

concentration, $V_{cmax\,25}$ increased 1.5-fold and g_{sw} twofold. N_{area} showed a significant association with soil P concentration but with little explanatory power ($R^2 = 0.02$; Figure 4g).

Species at low-MAP sites (especially at MAP <1000 mm) tended to have higher N_{area} ($R^2 = 0.37$; Figure 5g), which was by far the strongest correlation in this part of our analysis. The higher N_{area} at low rainfall corresponded (as expected) to higher $V_{cmax\,25}$ ($R^2 = 0.11$; Figure 5d). By contrast, g_{sw} showed no relationship with MAP (Figure 5a). The N_{area}–MAP scaling slope of -0.39 indicates that for a tenfold decrease in MAP, N_{area} increased nearly 2.5-fold, on average. On average, there was a 1.5-fold increase in $V_{cmax\,25}$ over this same interval in MAP (log–log slope = -0.26). Species at
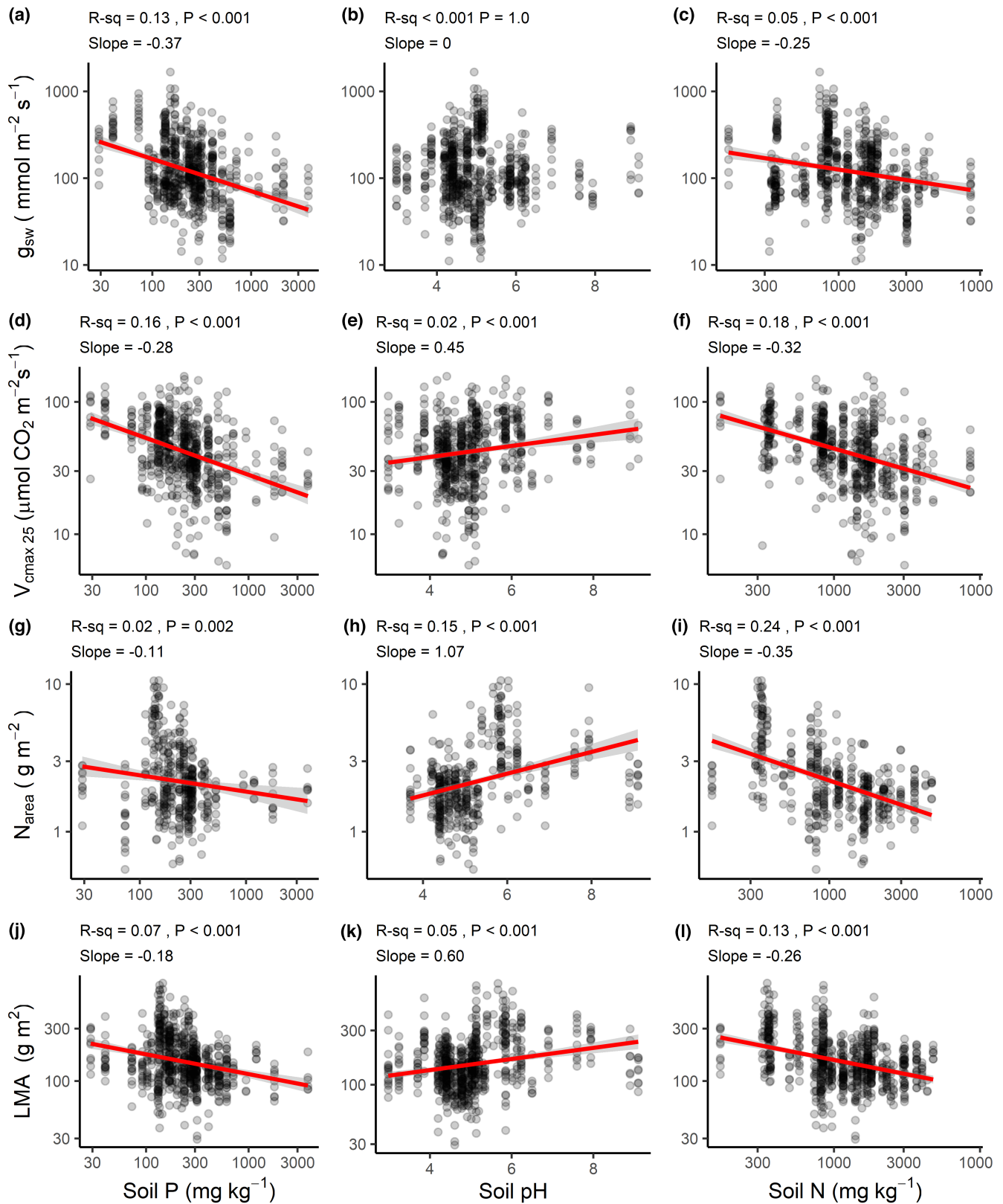
FIGURE 4 Trait–soil relationships from bivariate linear regression analysis. Points represent species-site means. All axes (except soil pH) have been $\log_{10}$-scaled. Abbreviations follow those in Table S1 and Figure 3. Red lines represent trend lines with 95% confidence intervals in gray and are only shown for statistically significant (*p*-values <.05, solid line). In panel (b), the slope coefficient was |<.005|.

warmer sites typically had higher g_{sw} but lower N_{area} (Figure 5b,h), consistent with the predicted and observed MAT effect on N_{area}–g_{sw} slopes (Figure 1, Figure 3). That said, there was pronounced

scatter in these relationships ($0.05 \leq R^2 \leq 0.07$). $V_{cmax\ 25}$ showed a marginally significant relationship with MAT (Figure 5f) but with <1% explanatory power.
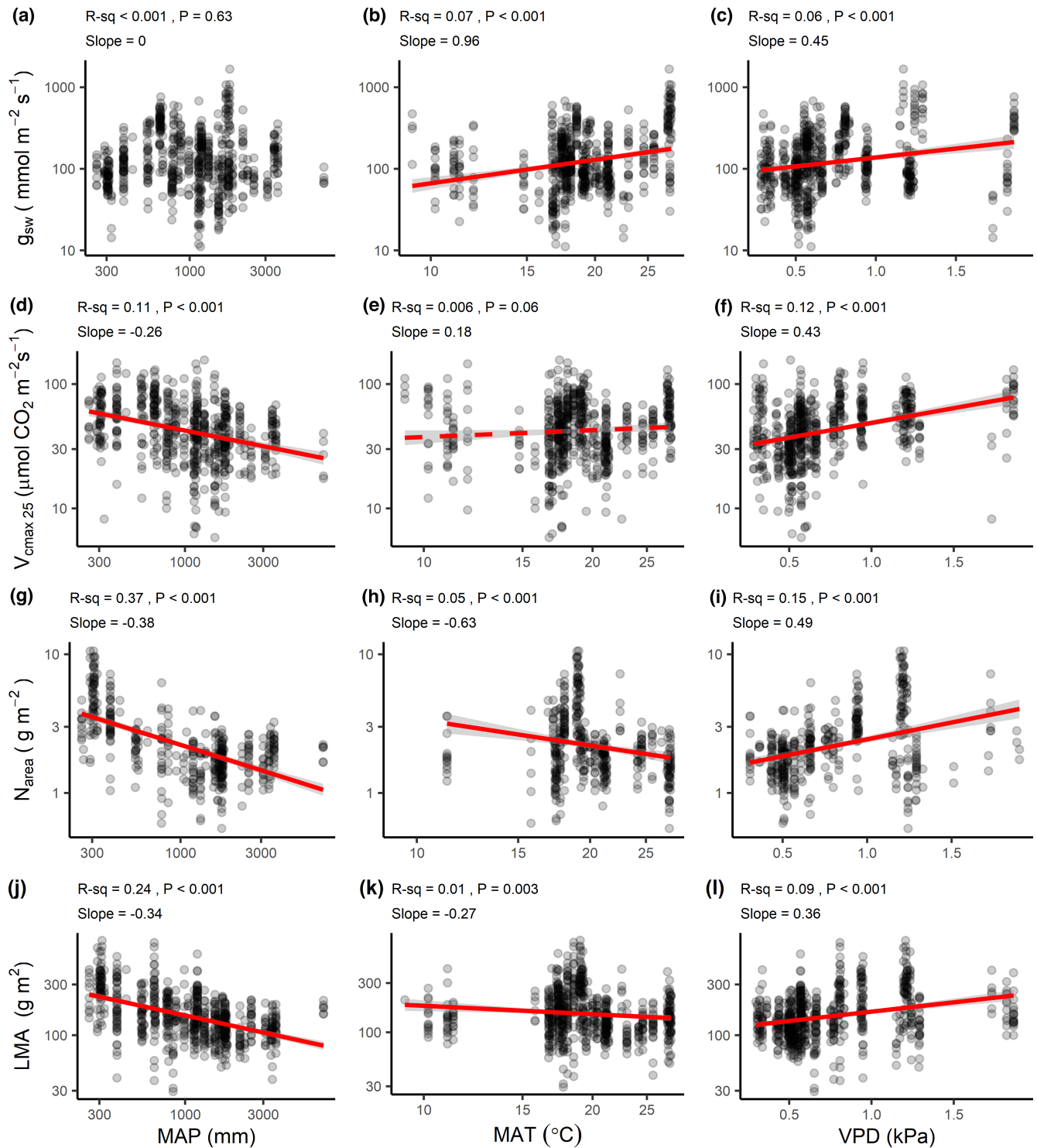
FIGURE 5 Trait–climate relationships from bivariate linear regression analysis. Points represent species-site means. All axes (except soil pH) have been log_{10}-scaled. Abbreviations follow those in Table S1 and Figure 3. Red lines represent trend lines with 95% confidence intervals in gray and are only shown for statistically significant ($p < .05$, solid line, $0.05 < p < .10$, dashed line). In panel (a), the slope coefficient was $|<.005|$.

Of the remaining soil variables (Table S4), BDW ($0.10 \leq R^2 \leq 0.21$), SOC ($0.01 \leq R^2 \leq 0.23$), and sand content ($0.01 \leq R^2 \leq 0.19$) explained the most variation in the focal traits. Of the remaining climate variables, the results were idiosyncratic but VPD explained a significant proportion of the trait variation ($0.06 \leq R^2 \leq 0.15$), as expected.

The partial regression analysis on the trait–environment relationships (Table S5) was largely similar to the OLS regression with a few exceptions. First, the effect of soil P on N_{area} was positive (rather than negative) when we accounted for the other abiotic variables. Second, there was a significant negative effect of soil pH on g_{sw} and

on C_i:C_a, where previously these relationships were not statistically significant.

4 | DISCUSSION

Despite the critical role of photosynthesis in driving the carbon cycle of terrestrial ecosystems, we understand relatively little about how soil fertility influences the coordination of photosynthetic traits, and the relative effects of soil versus climate. Here, we report the effects of a globally relevant, limiting soil nutrient, phosphorus (P), on photosynthetic trait coordination. Previously, for four sites in Australia, we reported trait shifts in relation to site temperature and aridity that were consistent with predictions from least-cost theory (Prentice et al., 2014; Wright et al., 2003). In a global study (Paillassa et al., 2020), we then examined the interactive effects of soil and climate, focusing on pH and soil texture as indices of fertility. Here we expand on the Australian study, including hundreds more species from many more sites (67), a much wider range of climate variables and, very importantly, we extend the analyses to soil nutrients.

4.1 | Climate effects

Using the largest Australian photosynthetic trait dataset to date, we generally observed that climate effects were stronger than soil effects. We report strong climate-driven trait shifts in line with previous studies and in line with our predictions. Most notably, with lower MAP we observed higher N_{area} and $V_{cmax\,25}$ at a given g_{sw}, higher N_{area} and $V_{cmax\,25}$ overall, and lower C_i:C_a. Although g_{sw} was not influenced by site precipitation, higher N_{area} and $V_{cmax\,25}$ drove the steeper N_{area}–g_{sw} and $V_{cmax\,25}$–g_{sw} slope relationships across the precipitation gradient. Steeper $V_{cmax\,25}$–g_{sw} and N_{area}–g_{sw} relationships at drier sites underlie the lower C_i:C_a in these places, the higher carboxylation capacity (at a given g_{sw}) drawing leaf-internal CO_2 down to lower concentrations. The lack of patterning of g_{sw} with respect to MAP accords with "global" results from Wright, Reich, et al. (2004) and Murray et al. (2019, 2020). The uncoupling of g_{sw} from MAP is interesting, as VPD is typically higher on more arid sites and g_{sw} increased with VPD (Table S4), indicating higher transpiration rates when stomata are open. Similar to the present study, global (Paillassa et al., 2020; Wang et al., 2017) and regional studies (Bloomfield et al., 2019; Cernusak, Hutley, et al., 2011; Cochrane et al., 2016; Wright et al., 2001) have reported lower C_i:C_a, higher $V_{cmax\,25}$, and higher leaf nutrient concentrations (especially per unit area) in drier habitats.

Least-cost theory predicts that MAT affects both water and carboxylation costs. In this study MAT effects matched our predictions but were weaker than those of MAP. Both the MAT and MAP effects were stronger than soil effects—at least in the bivariate relationships (see 4.2). These findings suggest that environmental variables that solely affect the unit costs of N (and carboxylation) exert weaker effects on photosynthetic trait coordination than do environmental

variables that influence the unit costs of water (i.e., MAP) or influence the costs of both water and carboxylation (i.e., MAT). Interestingly, we also observed weaker effects of MAT relative to MAP on the $V_{cmax\,25}$–g_{sw} and N_{area}–g_{sw} relationships—but not C_i:C_a—when considered in a multiple regression framework. The weaker effect size of MAT in the multiple regression likely resulted from collinearity between MAT and either soil pH ($r = 0.22$) or MAP ($r = 0.25$), the latter of which are often confounded, and can have compounding effects on plant functional traits. For example, globally, species growing on relatively dry sites tend to have small leaves when the mean temperature of the warmest month (TWM) is high, whereas species on wetter sites typically have larger leaves when TWM is high (Wright et al., 2017). From bivariate regressions, we also found that seasonality in temperature strongly (positively) influenced the N_{area}–g_{sw} and $V_{cmax\,25}$–g_{sw} slope relationships (Table S4), perhaps suggesting that more seasonal environments have higher water costs.

4.2 | Soil effects

Plants have various strategies that enhance their ability to cope with drought and nutrient deficiency, two properties that characterize much of the Australian continent. Indeed, a significant proportion of Australian plants possess scleromorphic long-lived leaves with low mass-based nutrient concentrations (Beadle, 1966; Lambers et al., 2010; Lamont, 1982; Specht, 1969; Wright et al., 2002; Wright, Groom, et al., 2004) and highly proficient nutrient resorption (Wright & Westoby, 2003). That is, most Australian plant species are generally positioned toward the "slow" end of the leaf economics spectrum (Wright, Reich, et al., 2004).

In this study we considered the effects of soil fertility via soil total P concentration and soil pH, both of which presumably influence the unit costs of N and carboxylation more so than water costs. Soil P concentration is a long-term site property that is strongly determined by parent material and is widely used as an indicator of soil P status in Australian ecology (Beadle, 1954, 1966; Fonseca et al., 2000; Kooyman et al., 2017). In contrast to soil total N concentration, which is quite stable across time, soil N and P availability can vary seasonally and also with plant nutrient-acquisition strategies, often reflecting root morphology, the tendency for carboxylate release and associations with mycorrhizal fungi (Lambers & Oliveira, 2019; Richardson et al., 2005; Turner, 2008). In the bivariate analyses (Figure 2), $V_{cmax\,25}$ and g_{sw} showed clear negative relationships with soil P concentration ($R^2 = 0.13$–0.16) and the soil P effect was far greater than the soil pH effect overall. Because all of g_{sw}, N_{area}, and $V_{cmax\,25}$ increased as soil P decreased, it makes sense that their ratios (the N_{area}–g_{sw} and $V_{cmax\,25}$–g_{sw} slopes) show little pattern over soil P gradients. The negative relationship between N_{area} and soil P in the OLS regression resulted from LMA being typically higher on low-P soils (Table S4) and in this study, there was a positive relationship between LMA and N_{area} ($r = 0.75$, $p < .001$, results not shown) and between N_{area} and $V_{cmax\,25}$ ($r = 0.37$, $p < .001$, results not shown). We note, however, that the relationship between N_{area} and soil P became positive when we accounted for the

effects of soil pH, MAP, and MAT (Table S5), which likely reflects the strong, negative effect of MAP on LMA and therefore N_{area}. A positive relationship between N_{area} and soil P was also observed in partial residual plots generated by Peng et al. (2021), which utilized a global dataset that included Australia.

The high $V_{cmax\ 25}$ at low soil P concentration is novel and unexpected, whereas the negative relationship between soil P and C_i:C_a matched predictions from least-cost theory (Tables S4 and S5). Least-cost theory also predicts that all else equal, C_i:C_a and $V_{cmax\ 25}$ should be inversely related (Wright et al., 2003), which we observed in the present study ($r = −0.15$, $p ≤ .001$, results not shown). In contrast to the $V_{cmax\ 25}$–soil P relationship, the g_{sw} effect was in line with our expectations: Maire et al. (2015) reported a negative association between plant-available soil P concentration and g_{sw}, arguing that nutrient deficiency promotes greater root production, increasing plant-available water and increasing g_{sw} and C_i:C_a. The authors also suggested that stimulation of transpiration (and g_{sw}) on nutrient-deficient sites may increase mass flow of soil nutrients to roots, ultimately enhancing leaf N and ultimately, $V_{cmax\ 25}$ [i.e., the mass-flow hypothesis (Cernusak, Winter, et al., 2011; Cramer et al., 2009; Edwards et al., 1998)]. Because the mobility of P is low compared with that of N, mass flow is more likely to increase N uptake than P uptake and may only increase P supply on P-impoverished, sandy soils with low P buffering capacity (Cernusak, Winter, et al., 2011; Huang et al., 2017).

Considering the importance of P for leaf metabolism, environmental properties that affect the per-unit cost of P acquisition from the soil arguably also affect the unit cost of carboxylation, vis-à-vis least-cost theory. The chief way that soil P is more expensive to acquire on low-P soils is in terms of higher belowground expenditure, for example, greater fine root production, greater expenditure supporting mycorrhizal symbionts, greater expenditure on root exudates that enhance access to recalcitrant pools of soil P (e.g., phosphatases; organic acids released by cluster roots), and greater expenditure on cluster roots (Raven et al., 2018). The latter are especially common in the Australian flora, particularly in the Proteaceae which exhibit very high photosynthetic phosphorus-use efficiency (PPUE) (Denton et al., 2007; Guilherme Pereira et al., 2019), that is, rapid photosynthetic rates at low leaf P concentrations (Lambers et al., 2012; Yan et al., 2019). In this study, we observed higher PPUE and higher PNUE for plants growing on low-P soils (Table S4) and higher $V_{cmax\ 25}$ on low-P soils. High PPUE may be accomplished by shifting allocation away from phospholipids toward galactolipids (the latter being a key component of chloroplast membranes) and sulfolipids that do not contain P (Lambers et al., 2012; Yan et al., 2019) with the transition from young to mature leaves. Interestingly, Australian Proteaceae growing on P-deficient soils have been shown to have low Rubisco activity but high levels of photosynthesis at low leaf P compared to *Arabidopsis* (Sulpice et al., 2014). The reduction in Rubisco activity likely resulted from a lower abundance of ribosomes and therefore lower rRNA levels, which may constrain the synthesis of proteins, including Rubisco. Thus, Australian plants appear to be well-adapted to low-P soils, as they maintain high levels of photosynthesis, high rates of carboxylation, and high photosynthetic nutrient-use efficiency in these environments.

Soil pH alters the solubility of soil minerals and causes shifts in community composition of soil bacteria (Lauber et al., 2008), which in turn affects nutrient availability. We thus included soil pH alongside soil total P concentration, due to its potential effects on the unit cost of carboxylation. Against expectation, variation in soil pH had negligible effects on the N_{area}–g_{sw} and $V_{cmax\ 25}$–g_{sw} relationships but C_i:C_a did decrease with increasing pH, albeit weakly ($R^2 = 0.03$), as predicted. While the pH effects were weak to negligible, the pattern in C_i:C_a matched global studies that showed strong modulation of N_{area}–g_{sw} and $V_{cmax\ 25}$–g_{sw} relationships, C_i:C_a and $\Delta^{13}C$ via soil pH (Cornwell et al., 2018; Paillassa et al., 2020; Wang et al., 2017). C_i:C_a is tightly determined by the balance between $V_{cmax\ 25}$ and g_{sw}, such that the $V_{cmax\ 25}$–g_{sw} relationship is a function of the optimal C_i:C_a, which is itself a function of water and N costs (Prentice et al., 2014). Therefore, it is possible that C_i:C_a better reflects costs associated with soil and climate properties than do the slopes, as it more directly integrates N and water costs. This is evidenced by the observation that C_i:C_a was sensitive (statistically significant) to all four of the chosen environmental variables whether analyzed in bivariate regressions or multiple regression. Although N_{area} was strongly influenced by soil pH ($R^2 = 0.15$), g_{sw} was not (Figure 4) and $V_{cmax\ 25}$ was only weakly affected ($R^2 = 0.02$). The positive effect of pH on leaf N concentration suggests moderately higher soil nutrient availability in less acidic soils, despite the negligible effect of soil pH on the $V_{cmax\ 25}$–g_{sw} and N_{area}–g_{sw} slopes. Maire et al. (2015) also found no relationship between g_{sw} and soil pH in a global study and in general, the soil pH effects in this study were considerably weaker than those reported at global scale (cf. Paillassa et al., 2020).

While the weak pH effects in the present study were unexpected, this suggests that soil pH may not be an especially useful index of nutrient-acquisition costs in low-fertility landscapes. We note that the partial regression analyses resulted in a statistically significant negative effect of soil pH on g_{sw} and C_i:C_a, the latter of which matched our predictions, indicating strong collinearities among the predictors. Nevertheless, soil pH does not underlie variation in photosynthetic traits within this system to the extent that soil P does. The finding that climate has a greater role in photosynthetic trait coordination than soil pH contrasts with the findings of our companion study (Paillassa et al., 2020), and may reflect the predominance of low pH/low-nutrient sites in our Australian dataset (only 4 of 67 sites with pH >7).

4.3 | Implications for global studies

By improving our understanding of photosynthetic trait–environment relationships at the regional and global scale, there is the potential to enhance the conceptual basis and parameterization of global vegetation models. For example, dynamic global

vegetation models (DGVMs) rarely incorporate variation in eco-physiological traits within plant functional types (e.g., across species or populations) or include environmental dependencies of traits (Grimm et al., 2017; Scheiter et al., 2013; Verheijen et al., 2013; Yang et al., 2015). We have now demonstrated that soil properties, namely soil P concentration and soil pH (Maire et al., 2015; Paillassa et al., 2020), influence the coordination of ecophysiological traits at a continental scale. These findings support increasing calls for soil properties to be included in vegetation models (Norby et al., 2017) and could be further developed using least-cost theory.

Within the least-cost theory framework, the first-order costs are set by site properties, whole-plant respiration rates, and tissue chemistry (e.g., leaf N or Rubisco concentration). In the formulation of least-cost theory by Prentice et al. (2014), optimal C_i:C_a is proportional to the ratio of two dimensionless parameters, *a* and *b*, which reflect the maintenance respiration costs of transpiration and carboxylation, respectively. Paillassa et al. (2020) re-expressed the cost functions to incorporate the effects of soil N and water supply, surmising that maintenance respiration costs at a given transpiration rate or carboxylation rate should increase when soil water or nutrients are scarce. But, of course, these are necessary simplifications that do not account for all relevant costs. Most importantly, water and nutrient unit costs are presumably also affected by species life history traits. For example, information regarding inter- and intra-specific variation in the ability to acquire soil water or nutrients via alternative allocation or acquisition strategies, including root activity and depth, nutrient-acquisition strategies (e.g., cluster roots vs. N_2 fixation vs. mycorrhizal symbioses; Lambers et al., 2008), and wood permeability (Wright et al., 2003), would likely help in the interpretation of within-site variation in photosynthetic traits. For example, mycorrhizal species may have lower N costs than non-mycorrhizal species, which would result in higher N_{area} for a given g_{sw} in the mycorrhizal species. Regions dominated by mycorrhizal species are thus expected to have species with higher N_{area}–g_{sw} slopes than regions where such species are absent, even when these occur at similar soil nutrient levels.

Additional considerations are needed before we can quantitatively integrate the effects of concentrations of soil P (or other metrics of fertility) in DGVMs. For example, one can make assumptions about the extent to which different nutrients are *substitutable* [e.g., whether species can "spend" more N belowground by investing in phosphatase enzymes to obtain more soil P (Olander & Vitousek, 2000; Schleuss et al., 2020; Treseder & Vitousek, 2001)], or simply *coordinated*, and specify nutrient exchange rates in a currency that can also be applied to water costs. It is also worth considering how additional soil properties influence soil nutrient costs, as soil texture, which influences both the availability of nutrients and water, seems also important for understanding geographic variation in photosynthetic trait coordination (Paillassa et al., 2020). For example, soils with higher silt content can hold more water than sandy soils, reducing water costs, such that plants typically have higher g_{sw}

coupled with higher $V_{cmax\,25}$ on silty soils (Paillassa et al., 2020). In this study, we found that plants growing on silt-rich soils had higher g_{sw} and higher N_{area} and $V_{cmax\,25}$, but similar slope relationships (Table S4), indicating a proportional increase in these traits, which canceled out. We also found a positive relationship between soil effective cation exchange capacity (ECE) and the slope relationships, indicating that nutrient costs were lower with increasing ECE, which is positively associated with soil nutrient availability. Lastly, we acknowledge the important role of soil N in other regions of the world, which significantly influenced individual photosynthetic traits (with the exception of C_i:C_a) but not trait coordination in this study system. The negative relationship between leaf N and soil total N, which was also reported by Maire et al. (2015), may result from low plant-available N if the soil organic matter has a high C:N ratio (Parton et al., 1988). Further consideration of long- versus short-term indices of soil resources is also warranted. Here we focused on evolutionary adaptations to soil nutrient pools rather than on acclimation to soil nutrient availabilities that can vary tremendously over relatively short timescales. Future studies could consider the relative strengths of short- and long-term controls on photosynthetic trait coordination, as this would be useful for quantifying within-species variation in trait relationships.

5 | CONCLUSIONS

Rainfall and temperature are expected to change considerably over the coming decades, regionally and globally, altering the availabilities of soil nutrients. While much is known regarding how climate drives variation in photosynthesis, few studies have investigated soil effects, although this is changing. Among our findings, the coordination of photosynthetic traits in response to soil P concentration is especially novel, as it suggests a unique contribution of a limiting soil nutrient that is independent of climate and soil pH. The simple theoretical framework known as least-cost theory can thus be applied to low-nutrient regions globally, for example, highly weathered soils and tropical regions, where P limits productivity. By considering the dependencies of plant traits on both climate and soils, we will better understand the proximate and long-term controls of photosynthesis.

CONFLICT OF INTEREST

The authors declare no conflicts of interest.

DATA AVAILABILITY STATEMENT

The data that support the findings of this study are openly available in Dryad at https://doi.org/10.5061/dryad.j9kd51cgr.

ORCID

Andrea C. Westerband https://orcid.org/0000-0003-4065-9689
Ian J. Wright https://orcid.org/0000-0001-8338-9143
Vincent Maire https://orcid.org/0000-0002-3245-2568
Jennifer Paillassa https://orcid.org/0000-0002-0683-4693
Iain Colin Prentice https://orcid.org/0000-0002-1296-6764
Owen K. Atkin https://orcid.org/0000-0003-1041-5202
Lucas A. Cernusak https://orcid.org/0000-0002-7575-5526
Ning Dong https://orcid.org/0000-0003-0793-8854
Sean M. Gleason https://orcid.org/0000-0002-5607-4741
Caio Guilherme Pereira https://orcid.org/0000-0003-3288-8553
Hans Lambers https://orcid.org/0000-0002-4118-2272
Michelle R. Leishman https://orcid.org/0000-0003-4830-5797
Yadvinder Malhi https://orcid.org/0000-0002-3503-4783
Rachael H. Nolan https://orcid.org/0000-0001-9277-5142

REFERENCES

Beadle, N. (1954). Soil phosphate and the delimitation of plant communities in eastern Australia. *Ecology*, 35(3), 370–375.

Beadle, N. (1966). Soil phosphate and its role in molding segments of the Australian flora and vegetation, with special reference to xeromorphy and sclerophylly. *Ecology*, 47(6), 992–1007.

Bloomfield, K. J., Cernusak, L. A., Eamus, D., Ellsworth, D. S., Prentice, I. C., Wright, I. J., Boer, M. M., Bradford, M. G., Cale, P., Cleverly, J., Egerton, J. J. G., Evans, B. J., Hayes, L. S., Hutchinson, M. F., Liddell, M. J., Macfarlane, C., Meyer, W. S., Prober, S. M., Togashi, H. F., … Atkin, O. K. (2018). A continental-scale assessment of variability in leaf traits: Within species, across sites and between seasons. *Functional Ecology*, 32(6), 1492–1506.

Bloomfield, K. J., Prentice, I. C., Cernusak, L. A., Eamus, D., Medlyn, B. E., Rumman, R., Wright, I. J., Boer, M. M., Cale, P., Cleverly, J., Egerton, J. J. G., Ellsworth, D. S., Evans, B. J., Hayes, L. S., Hutchinson, M. F., Liddell, M. J., Macfarlane, C., Meyer, W. S., Togashi, H. F., … Atkin, O. K. (2019). The validity of optimal leaf traits modelled on environmental conditions. *New Phytologist*, 221(3), 1409–1423.

Cernusak, L. A., Hutley, L. B., Beringer, J., Holtum, J. A., & Turner, B. L. (2011). Photosynthetic physiology of eucalypts along a sub-continental rainfall gradient in northern Australia. *Agricultural and Forest Meteorology*, 151(11), 1462–1470.

Cernusak, L. A., Winter, K., & Turner, B. L. (2011). Transpiration modulates phosphorus acquisition in tropical tree seedlings. *Tree Physiology*, 31(8), 878–885.

Chen, J. L., Reynolds, J. F., Harley, P. C., & Tenhunen, J. D. (1993). Coordination theory of leaf nitrogen distribution in a canopy. *Oecologia*, 93(1), 63–69. https://doi.org/10.1007/bf00321192

Cochrane, A., Hoyle, G. L., Yates, C. J., Neeman, T., & Nicotra, A. B. (2016). Variation in plant functional traits across and within four species of Western Australian Banksia (Proteaceae) along a natural climate gradient. *Austral Ecology*, 41(8), 886–896.

Cornwell, W. K., Wright, I. J., Turner, J., Maire, V., Barbour, M. M., Cernusak, L. A., Dawson, T., Ellsworth, D., Farquhar, G. D., Griffiths, H., Keitel, C., Knohl, A., Reich, P. B., Williams, D. G., Bhaskar, R., Cornelissen, J. H. C., Richards, A., Schmidt, S., Valladares, F., … Santiago, L. S. (2018). Climate and soils together regulate photosynthetic carbon isotope discrimination within C3 plants worldwide. *Global Ecology and Biogeography*, 27(9), 1056–1067. https://doi.org/10.1111/geb.12764

Courville, T., & Thompson, B. (2001). Use of structure coefficients in published multiple regression articles: beta is not enough. *Educational and Psychological Measurement*, 61(2), 229–248. https://doi.org/10.1177/0013164401612006

Cramer, M. D., Hawkins, H. J., & Verboom, G. A. (2009). The importance of nutritional regulation of plant water flux. *Oecologia*, 161(1), 15–24.

de Caritat, P., Cooper, M., & Wilford, J. (2011). The pH of Australian soils: Field results from a national survey. *Soil Research*, 49(2), 173–182.

De Kauwe, M. G., Lin, Y. S., Wright, I. J., Medlyn, B. E., Crous, K. Y., Ellsworth, D. S., Maire, V., Prentice, I. C., Atkin, O. K., Rogers, A., Niinemets, U., Serbin, S. P., Meir, P., Uddling, J., Togashi, H. F., Tarvainen, L., Weerasinghe, L. K., Evans, B. J., Ishida, F. Y., & Domingues, T. F. (2016). A test of the 'one-point method'for estimating maximum carboxylation capacity from field-measured, light-saturated photosynthesis. *New Phytologist*, 210(3), 1130–1144.

Denton, M. D., Veneklaas, E. J., Freimoser, F. M., & Lambers, H. (2007). Banksia species (Proteaceae) from severely phosphorus-impoverished soils exhibit extreme efficiency in the use and re-mobilization of phosphorus. *Plant, Cell & Environment*, 30(12), 1557–1565.

Domingues, T. F., Meir, P., Feldpausch, T. R., Saiz, G., Veenendaal, E. M., Schrodt, F., Bird, M., Djagbletey, G., Hien, F., Compaore, H., Diallo, A., Grace, J., & Lloyd, J. (2010). Co-limitation of photosynthetic capacity by nitrogen and phosphorus in West Africa woodlands. *Plant, Cell & Environment*, 33(6), 959–980.

Dong, N., Prentice, I. C., Evans, B. J., Caddy-Retalic, S., Lowe, A. J., & Wright, I. J. (2017). Leaf nitrogen from first principles: field evidence for adaptive variation with climate. *Biogeosciences*, 14(2), 481–495. https://doi.org/10.5194/bg-14-481-2017

Dong, N., Prentice, I. C., Wright, I. J., Evans, B. J., Togashi, H. F., Caddy-Retalic, S., McInerney, F. A., Sparrow, B., Leitch, E., & Lowe, A. J. (2020). Components of leaf-trait variation along environmental gradients. *New Phytologist*, 228(1), 82–94.

Dong, N., Wright, I. J., Chen, J. M., Luo, X., Wang, H., Keenan, T. F., Smith, N. G., & Prentice, I. C. (2022). Rising CO_2 and warming reduce global canopy demand for nitrogen. *New Phytologist*, 235(5), 1692–1700.

Eamus, D., & Prichard, H. (1998). A cost-benefit analysis of leaves of four Australian savanna species. *Tree Physiology*, 18(8-9), 537–545. https://doi.org/10.1093/treephys/18.8-9.537

Edwards, D., Kerp, H., & Hass, H. (1998). Stomata in early land plants: an anatomical and ecophysiological approach. *Journal of Experimental Botany*, 255–278.

Farquhar, G. D., von Caemmerer, S. V., & Berry, J. A. (1980). A biochemical model of photosynthetic CO_2 assimilation in leaves of C3 species. *Planta*, 149(1), 78–90.

Field, C., Merino, J., & Mooney, H. A. (1983). Compromises between water-use efficiency and nitrogen-use efficiency in 5 species of California evergreens. *Oecologia*, 60(3), 384–389. https://doi.org/10.1007/bf00376856

Fierer, N., & Jackson, R. B. (2006). The diversity and biogeography of soil bacterial communities. *Proceedings of the National Academy of Sciences*, 103(3), 626–631.

Fonseca, C. R., Overton, J. M., Collins, B., & Westoby, M. (2000). Shifts in trait-combinations along rainfall and phosphorus gradients. *Journal of Ecology*, 88(6), 964–977.

Friend, A. D., Geider, R. J., Behrenfeld, M. J., & Still, C. J. (2009). Photosynthesis in global-scale models. In A. Laisk, L. Nedbal & Govindjee (Eds.), *Photosynthesis in silico* (pp. 465–497). Advances in Photosynthesis and Respiration, Vol. 29. Springer. https://doi.org/10.1007/978-1-4020-9237-4_20

Grimm, V., Ayllón, D., & Railsback, S. F. (2017). Next-generation individual-based models integrate biodiversity and ecosystems: yes we can, and yes we must. *Ecosystems*, 20(2), 229–236.

Grundy, M. J., Rossel, R. A. V., Searle, R. D., Wilson, P. L., Chen, C., & Gregory, L. J. (2015). Soil and Landscape Grid of Australia. *Soil Research*, 53(8), 835–844. https://doi.org/10.1071/SR15191

Guilherme Pereira, C., Hayes, P. E., O'Sullivan, O. S., Weerasinghe, L. K., Clode, P. L., Atkin, O. K., & Lambers, H. (2019). Trait convergence in photosynthetic nutrient-use efficiency along a 2-million year dune chronosequence in a global biodiversity hotspot. *Journal of Ecology*, 107(4), 2006–2023.

He, X., Augusto, L., Goll, D. S., Ringeval, B., Wang, Y., Helfenstein, J., Huang, Y., Yu, K., Wang, Z., Yang, Y., & Hou, E. (2021). Global patterns and drivers of soil total phosphorus concentration. *Earth System Science Data*, 13(12), 5831–5846.

Hikosaka, K., Nabeshima, E., & Hiura, T. (2007). Seasonal changes in the temperature response of photosynthesis in canopy leaves of Quercus crispula in a cool-temperate forest. *Tree Physiology*, 27(7), 1035–1041.

Huang, G., Hayes, P. E., Ryan, M. H., Pang, J., & Lambers, H. (2017). Peppermint trees shift their phosphorus-acquisition strategy along a strong gradient of plant-available phosphorus by increasing their transpiration at very low phosphorus availability. *Oecologia*, 185(3), 387–400.

Hutchinson, M. F., McKenney, D. W., Lawrence, K., Pedlar, J. H., Hopkinson, R. F., Milewska, E., & Papadopol, P. (2009). Development and testing of Canada-wide interpolated spatial models of daily minimum-maximum temperature and precipitation for 1961-2003. *Journal of Applied Meteorology and Climatology*, 48(4), 725–741. https://doi.org/10.1175/2008jamc1979.1

Kooyman, R. M., Laffan, S. W., & Westoby, M. (2017). The incidence of low phosphorus soils in Australia. *Plant and Soil*, 412(1-2), 143–150.

Körner, C., Farquhar, G., & Wong, S. (1991). Carbon isotope discrimination by plants follows latitudinal and altitudinal trends. *Oecologia*, 88(1), 30–40.

Laliberté, E., Zemunik, G., & Turner, B. L. (2014). Environmental filtering explains variation in plant diversity along resource gradients. *Science*, 345(6204), 1602–1605.

Lambers, H., Brundrett, M. C., Raven, J. A., & Hopper, S. D. (2010). Plant mineral nutrition in ancient landscapes: high plant species diversity on infertile soils is linked to functional diversity for nutritional strategies. *Plant and Soil*, 334, 11–31. https://doi.org/10.1007/s11104-010-0444-9

Lambers, H., Cawthray, G. R., Giavalisco, P., Kuo, J., Laliberté, E., Pearse, S. J., Scheible, W. R., Stitt, M., Teste, F., & Turner, B. L. (2012). Proteaceae from severely phosphorus-impoverished soils extensively replace phospholipids with galactolipids and sulfolipids during leaf development to achieve a high photosynthetic phosphorus-use-efficiency. *New Phytologist*, 196(4), 1098–1108.

Lambers, H., & Oliveira, R. (2019). *Plant physiological ecology* (3rd ed.). Springer Nature Switzerland AG.

Lambers, H., Raven, J. A., Shaver, G. R., & Smith, S. E. (2008). Plant nutrient-acquisition strategies change with soil age. *Trends in ecology & evolution*, 23(2), 95–103.

Lamont, B. (1982). Mechanisms for enhancing nutrient uptake in plants, with particular reference to mediterranean South Africa and Western Australia. *The Botanical Review*, 48(3), 597–689.

Lauber, C. L., Strickland, M. S., Bradford, M. A., & Fierer, N. (2008). The influence of soil properties on the structure of bacterial and fungal communities across land-use types. *Soil Biology and Biochemistry*, 40(9), 2407–2415.

Lin, Y.-S., Medlyn, B. E., De Kauwe, M. G., & Ellsworth, D. S. (2013). Biochemical photosynthetic responses to temperature: how do interspecific differences compare with seasonal shifts? *Tree Physiology*, 33(8), 793–806.

Maire, V., Martre, P., Kattge, J., Gastal, F., Esser, G., Fontaine, S., & Soussana, J. F. (2012). The coordination of leaf photosynthesis links C and N fluxes in C3 plant species. *Plos One*, 7(6), 15. https://doi.org/10.1371/journal.pone.0038345

Maire, V., Wright, I. J., Prentice, I. C., Batjes, N. H., Bhaskar, R., van Bodegom, P. M., Cornwell, W. K., Ellsworth, D., Niinemets, Ü., Ordonez, A., Reich, P. B., & Santiago, L. S. (2015). Global effects of soil and climate on leaf photosynthetic traits and rates. *Global Ecology and Biogeography*, 24(6), 706–717.

Murray, M., Soh, W. K., Yiotis, C., Batke, S., Parnell, A. C., Spicer, R. A., Lawson, T., Caballero, R., Wright, I. J., Purcell, C., & McElwain, J. C. (2019). Convergence in Maximum Stomatal Conductance of C-3 Woody Angiosperms in Natural Ecosystems Across Bioclimatic Zones. *Frontiers in Plant Science*, 10, 1–20. https://doi.org/10.3389/fpls.2019.00558

Murray, M., Soh, W. K., Yiotis, C., Spicer, R. A., Lawson, T., & McElwain, J. C. (2020). Consistent relationship between field-measured stomatal conductance and theoretical maximum stomatal conductance in C3 woody angiosperms in four major biomes. *International Journal of Plant Sciences*, 181(1), 142–154. https://doi.org/10.1086/706260

Norby, R. J., Gu, L., Haworth, I. C., Jensen, A. M., Turner, B. L., Walker, A. P., Warren, J. M., Weston, D. J., Xu, C., & Winter, K. (2017). Informing models through empirical relationships between foliar phosphorus, nitrogen and photosynthesis across diverse woody species in tropical forests of Panama. *New Phytologist*, 215(4), 1425–1437.

Northcote, H. K., & Wright, M. J. (1982). Soil landscapes of arid Australia. In *Evolution of the flora and fauna of arid Australia* (pp. 15–21). Peacock Publications.

Olander, L. P., & Vitousek, P. M. (2000). Regulation of soil phosphatase and chitinase activity by N and P availability. *Biogeochemistry*, 49(2), 175–191.

Ordoñez, J. C., Van Bodegom, P. M., Witte, J. P. M., Wright, I. J., Reich, P. B., & Aerts, R. (2009). A global study of relationships between leaf traits, climate and soil measures of nutrient fertility. *Global Ecology and Biogeography*, 18(2), 137–149.

Paillassa, J., Wright, I. J., Prentice, I. C., Pepin, S., Smith, N. G., Ethier, G., Westerband, A. C., Lamarque, L. J., Han, W., Cornwell, W. K., & Maire, V. (2020). When and where soil is important to modify the carbon and water economy of leaves. *New Phytologist*, 228(1), 121–135. https://doi.org/10.1111/nph.16702

Parton, W. J., Stewart, J. W., & Cole, C. V. (1988). Dynamics of C, N, P and S in grassland soils: a model. *Biogeochemistry*, 5(1), 109–131.

Pedhazur, E. J. (1997). *Multiple regression in behavioral research: Explanation and prediction* (3rd ed.). Harcourt Brace College Publishers.

Peng, Y., Bloomfield, K. J., Cernusak, L. A., Domingues, T. F., & Colin Prentice, I. (2021). Global climate and nutrient controls of photosynthetic capacity. *Communications Biology*, 4(1), 462. https://doi.org/10.1038/s42003-021-01985-7

Prentice, I. C., Dong, N., Gleason, S. M., Maire, V., & Wright, I. J. (2014). Balancing the costs of carbon gain and water transport: testing a new theoretical framework for plant functional ecology. *Ecology Letters*, 17(1), 82–91.

Prentice, I. C., Meng, T., Wang, H., Harrison, S. P., Ni, J., & Wang, G. (2011). Evidence of a universal scaling relationship for leaf CO_2 drawdown along an aridity gradient. *New Phytologist*, 190(1), 169–180.

R Development Core Team. (2017). *R: A language and environment for statistical computing*. R Foundation for Statistical Computing.

Raven, J. A., Lambers, H., Smith, S. E., & Westoby, M. (2018). Costs of acquiring phosphorus by vascular land plants: patterns and implications for plant coexistence. *New Phytologist*, 217(4), 1420–1427.

Rayment, G., & Lyons, D. (2011). *Soil chemical methods: Australasia*. CSIRO Publishing.

Reich, P. B., Oleksyn, J., & Wright, I. J. (2009). Leaf phosphorus influences the photosynthesis-nitrogen relation: a cross-biome analysis of 314 species. *Oecologia*, 160(2), 207–212. https://doi.org/10.1007/s00442-009-1291-3

Richardson, A., George, T., Hens, M., & Simpson, R. (2005). Utilization of soil organic phosphorus by higher plants. In B. Turner, E. Frossard, & D. Baldwin (Eds.), *Organic phosphorus in the environment* (pp. 165–184). CABI Publishing.

Scafaro, A. P., Xiang, S., Long, B. M., Bahar, N. H., Weerasinghe, L. K., Creek, D., Evans, J. R., Reich, P. B., & Atkin, O. K. (2017). Strong thermal acclimation of photosynthesis in tropical and temperate wet-forest tree species: The importance of altered Rubisco content. *Global Change Biology*, 23(7), 2783–2800.

Scheiter, S., Langan, L., & Higgins, S. I. (2013). Next-generation dynamic global vegetation models: learning from community ecology. *New Phytologist*, 198(3), 957–969.

Schleuss, P. M., Widdig, M., Heintz-Buschart, A., Kirkman, K., & Spohn, M. (2020). Interactions of nitrogen and phosphorus cycling promote P acquisition and explain synergistic plant-growth responses. *Ecology*, 101(5), e03003.

Sinsabaugh, R. L., & Follstad Shah, J. J. (2012). Ecoenzymatic stoichiometry and ecological theory. *Annual Review of Ecology, Evolution, and Systematics*, 43, 313–343.

Sinsabaugh, R. L., Lauber, C. L., Weintraub, M. N., Ahmed, B., Allison, S. D., Crenshaw, C., Contosta, A. R., Cusack, D., Frey, S., Gallo, M. E., Gartner, T. B., Hobbie, S. E., Holland, K., Keeler, B. L., Powers, J. S., Stursova, M., Takacs-Vesbach, C., Waldrop, M. P., Wallenstein, M. D., … Zeglin, L. H. (2008). Stoichiometry of soil enzyme activity at global scale. *Ecology letters*, 11(11), 1252–1264. https://doi.org/10.1111/j.1461-0248.2008.01245.x

Slessarev, E. W., Lin, Y., Bingham, N. L., Johnson, J. E., Dai, Y., Schimel, J. P., & Chadwick, O. A. (2016). Water balance creates a threshold in soil pH at the global scale. *Nature*, 540(7634), 567–569. https://doi.org/10.1038/nature20139

Smith, N. G., & Dukes, J. S. (2013). Plant respiration and photosynthesis in global-scale models: incorporating acclimation to temperature and CO_2. *Global Change Biology*, 19(1), 45–63.

Smith, N. G., Keenan, T. F., Colin Prentice, I., Wang, H., Wright, I. J., Niinemets, Ü., Crous, K. Y., Domingues, T. F., Guerrieri, R., Yoko Ishida, F., Kattge, J., Kruger, E. L., Maire, V., Rogers, A., Serbin, S. P., Tarvainen, L., Togashi, H. F., Townsend, P. A., Wang, M., … Zhou, S.-X. (2019). Global photosynthetic capacity is optimized to the environment. *Ecology letters*, 22(3), 506–517. https://doi.org/10.1111/ele.13210

Smith, S. D., Monson, R. K., & Anderson, J. E. (1997). *Physiological ecology of North American desert plants*. Springer.

Specht, R. (1969). A comparison of the sclerophyllous vegetation characteristic of Mediterranean type climates in France, California,

and Southern Australia. I. Structure, morphology, and succession. *Australian Journal of Botany*, 17(2), 277–292. https://doi.org/10.1071/BT9690277

Sulpice, R., Ishihara, H., Schlereth, A., Cawthray, G. R., Encke, B., Giavalisco, P., Ivakov, A., Arrivault, S., Jost, R., Krohn, N., Kuo, J., Laliberte, E., Pearse, S. J., Raven, J. A., Scheible, W.-R., Teste, F., Veneklaas, E. J., Stitt, M., & Lambers, H. (2014). Low levels of ribosomal RNA partly account for the very high photosynthetic phosphorus-use efficiency of Proteaceae species. *Plant, Cell & Environment*, 37(6), 1276–1298.

Taylor, G. (1994). Landscapes of Australia: Their nature and evolution. In *History of the Australian vegetation: Cretaceous to recent* (pp. 60–79). University of Adelaide Press.

Thornthwaite, C. W. (1948). An approach toward a rational classification of climate. *Geographical review*, 38(1), 55–94.

Togashi, H. F., Prentice, I. C., Atkin, O. K., Macfarlane, C., Prober, S. M., Bloomfield, K. J., & Evans, B. J. (2018). Thermal acclimation of leaf photosynthetic traits in an evergreen woodland, consistent with the coordination hypothesis. *Biogeosciences*, 15(11), 3461–3474.

Treseder, K. K., & Vitousek, P. M. (2001). Effects of soil nutrient availability on investment in acquisition of N and P in Hawaiian rain forests. *Ecology*, 82(4), 946–954.

Turner, B. L. (2008). Resource partitioning for soil phosphorus: a hypothesis. *Journal of Ecology*, 96(4), 698–702. https://doi.org/10.1111/j.1365-2745.2008.01384.x

Verheijen, L., Brövkin, V., Aerts, R., Bonisch, G., Cornelissen, J. H., Kattge, J., Reich, P. B., Wright, I. J., & Van Bodegom, P. (2013). Impacts of trait variation through observed trait-climate relationships on performance of an Earth system model: a conceptual analysis. *Biogeosciences*, 10, 5497–5515.

Viscarra Rossel, R., Chen, C., Grundy, M., Searle, R., Clifford, D., Odgers, N., Holmes, K., Griffin, T., Liddicoat, C., & Kidd, D. (2014). *Soil and Landscape Grid National Soil Attribute Maps Release 1* (Vol. v. 3). Collection 10.4225/08/546F540FE10AA.

Viscarra Rossel, R. A., & Bui, E. N. (2016). A new detailed map of total phosphorus stocks in Australian soil. *Science of the Total Environment*, 542, 1040–1049.

Vitousek, P. M. (1984). Litterfall, nutrient cycling, and nutrient limitation in tropical forests. *Ecology*, 65(1), 285–298.

Von Caemmerer, S., & Farquhar, G. D. (1981). Some relationships between the biochemistry of photosynthesis and the gas exchange of leaves. *Planta*, 153(4), 376–387.

Wang, H., Prentice, I. C., Keenan, T. F., Davis, T. W., Wright, I. J., Cornwell, W. K., Evans, B. J., & Peng, C. (2017). Towards a universal model for carbon dioxide uptake by plants. *Nature Plants*, 3(9), 734–741. https://doi.org/10.1038/s41477-017-0006-8

Warton, D. I., Wright, I. J., Falster, D. S., & Westoby, M. (2006). Bivariate line-fitting methods for allometry. *Biological Reviews*, 81(2), 259–291. https://doi.org/10.1017/s1464793106007007

Wright, I. J., Dong, N., Maire, V., Prentice, I. C., Westoby, M., Díaz, S., Gallagher, R. V., Jacobs, B. F., Kooyman, R., Law, E. A., Leishman, M. R., Niinements, U., Reich, P., Sack, L., Villar, R., Wang, H., & Wilf, P. (2017). Global climatic drivers of leaf size. *Science*, 357(6354), 917–921.

Wright, I. J., Groom, P. K., Lamont, B. B., Poot, P., Prior, L. D., Reich, P. B., Schulze, E.-D., Veneklaas, E. J., & Westoby, M. (2004). Leaf trait relationships in Australian plant species. *Functional Plant Biology*, 31(5), 551–558.

Wright, I. J., Reich, P. B., Cornelissen, J. H. C., Falster, D. S., Groom, P. K., Hikosaka, K., Lee, W., Lusk, C. H., Niinemets, Ü., Oleksyn, J., Osada, N., Poorter, H., Warton, D. I., & Westoby, M. (2005). Modulation of leaf economic traits and trait relationships by climate. *Global Ecology and Biogeography*, 14(5), 411–421. https://doi.org/10.1111/j.1466-822x.2005.00172.x

Wright, I. J., Reich, P. B., & Westoby, M. (2001). Strategy shifts in leaf physiology, structure and nutrient content between species of

high-and low-rainfall and high-and low-nutrient habitats. *Functional Ecology*, *15*(4), 423–434.

Wright, I. J., Reich, P. B., & Westoby, M. (2003). Least-Cost input mixtures of water and nitrogen for photosynthesis. *The American Naturalist*, *161*(1), 98–111. https://doi.org/10.1086/344920

Wright, I. J., Reich, P. B., Westoby, M., Ackerly, D. D., Baruch, Z., Bongers, F., Cavender-Bares, J., Chapin, T., Cornelissen, J. H. C., Diemer, M., Flexas, J., Garnier, E., Groom, P. K., Gulias, J., Hikosaka, K., Lamont, B. B., Lee, T., Lee, W., … Villar, R. (2004). The worldwide leaf economics spectrum. *Nature*, *428*, 821–827. https://doi.org/10.1038/nature02403

Wright, I. J., & Westoby, M. (2003). Nutrient concentration, resorption and lifespan: leaf traits of Australian sclerophyll species. *Functional Ecology*, *17*(1), 10–19.

Wright, I. J., Westoby, M., & Reich, P. B. (2002). Convergence towards higher leaf mass per area in dry and nutrient-poor habitats has different consequences for leaf life span. *Journal of Ecology*, *90*(3), 534–543.

Xu, T., Han, W., Hutchinson, M., Pauwels, J., Whitley, R., & Evans, B. (2015). eMAST R-Package collection (Dataset). https://portal.tern.org.au/emast-r-package-collection/21637

Yan, L., Zhang, X., Han, Z., Pang, J., Lambers, H., & Finnegan, P. M. (2019). Responses of foliar phosphorus fractions to soil age are diverse along a 2 Myr dune chronosequence. *New Phytologist*, *223*(3), 1621–1633.

Yang, Y., Zhu, Q., Peng, C., Wang, H., & Chen, H. (2015). From plant functional types to plant functional traits: A new paradigm in modelling global vegetation dynamics. *Progress in Physical Geography*, *39*(4), 514–535.

SUPPORTING INFORMATION

Additional supporting information can be found online in the Supporting Information section at the end of this article.

How to cite this article: Westerband, A. C., Wright, I. J., Maire, V., Paillassa, J., Prentice, I. C., Atkin, O. K., Bloomfield, K. J., Cernusak, L. A., Dong, N., Gleason, S. M., Guilherme Pereira, C., Lambers, H., Leishman, M. R., Malhi, Y., & Nolan, R. H. (2022). Coordination of photosynthetic traits across soil and climate gradients. *Global Change Biology*, *00*, 1–18. https://doi.org/10.1111/gcb.16501